

# **Digital Nonrecursive FIR Filter Design Using Exponential Window**

**Ayman Nashwan Al-Dabbagh**

Submitted to the  
Institute of Graduate Studies and Research  
in partial fulfillment of the requirements for the Degree of

Master of Science  
in  
Computer Engineering

Eastern Mediterranean University  
October 2013  
Gazimağusa, North Cyprus

Approval of the Institute of Graduate Studies and Research

---

Prof. Dr. Elvan Yılmaz  
Director

I certify that this thesis satisfies the requirements as a thesis for the degree of Master of Science in Computer Engineering.

---

Prof. Dr. Işık Aybay  
Chair, Department of Computer Engineering

We certify that we have read this thesis and that in our opinion it is fully adequate in scope and quality as a thesis for the degree of Master of Science in Computer Engineering.

---

Prof. Dr. Hasan Kömürcügil  
Supervisor

---

Examining Committee

1. Prof. Dr. Hakan Altınçay

---

2. Prof. Dr. Hasan Kömürcügil

---

3. Assoc. Prof. Dr. Ekrem Varoğlu

---

## ABSTRACT

Recently it has been found that the Exponential window gives better side-lobe roll-off ratio compared with Kaiser window. That difference is important for some applications like beam forming, filter design, and speech processing. In this thesis, the design of digital non-recursive finite impulse response (FIR) filter by using Exponential window is proposed.

One of the most effective variables is the far-end stopband attenuation especially when the signal needed to be filtered has a great concentration of spectral energy. In a sub-band coding, the filter is intended to separate out various frequency bands for independent processing. When it is applied on speech, the far-end rejection of the energy in the stopband needs to be as higher as possible to make leakage of the energy from one band to another as lower as possible. Therefore, the designed filter should have special specifications which should provide better far-end stopband attenuation (amplitude of last ripple in stopband). Finding a digital filter that has a higher performance far-end stopband attenuation than Kaiser window is very valuable when the FIR filter constructed by the use of Kaiser window far-end stopband attenuation becomes better than the one constructed by the well-known adjustable windows, for instance, the special cases of Ultraspherical windows, Dolph-Chebyshev and Saramaki.

In this thesis, the construction of non-recursive digital FIR filter has been presented through applying Exponential window. After applying the Exponential window, it is found that the far-end stopband attenuation becomes better than the filter constructed

by Kaiser window, and that is one of the advantages of filter building by using Exponential window over Kaiser window. The proposed scheme is simulated by MATLAB. All the simulation results show a good agreement with the proposed theory.

**Keywords:** Digital FIR Filter, Side-lobe Roll-off Ratio, Far-end Stopband Attenuation, Window Technique, Kaiser Window, Exponential Window

## ÖZ

Son zamanlarda üstsel pencerenin Kaiser penceresine göre daha iyi kenar-lob yuvarlanma oranı verdiği bulunmuştur. Bu farklılık, demet yapımı, süzgeç tasarımı, ve konuşma işleme gibi bazı uygulamalarda önemlidir. Bu tezde, sonlu-dürtü-cevaplı (FIR) sayısal yinelemesiz süzgeç için üstsel pencere kullanarak tasarımı önerilmektedir.

Süzgeçlenecek sinyalin yoğun enerjisi olduğu durumlarda uzak-son durduran bant zayıflatma en önemli değişkenlerden bir tanesidir. Alt bant kodlamada, süzgecin çeşitli frekans bantlarını bağımsız işlem yaparak ayırması beklenir. Konuşmaya uygulandığı zaman, durdurma bandında enerjinin uzak-son kabul edilmemesi mümkün olduğu kadar yüksek olmalıdır. Dolayısıyla, tasarlanan süzgecin iyi uzak-son durduran bant zayıflatma gibi özel tarifnamesi olması gerekir. FIR süzgecin Kaiser penceresi ile tasarlandığı durumda, uzak-son durduran band zayıflaması iyi bilinen ayarlanabilir pencereler (Ultraspherical, Dolph-Chebyshev ve Saramaki) ile tasarlanan süzgeçlerden daha iyi olmaktadır.

Bu tezde, yinelemesiz sayısal FIR süzgecinin üstsel pencere kullanarak tasarımı önerilmiştir. Üstsel pencere uygulanması sonucu olarak, uzak-son durduran bant zayıflatmasının Kaiser penceresi ile elde edilenden daha iyi olduğu bulunmuştur. Önerilen yöntemin simülasyonu MATLAB yardımıyla yapılmıştır. Elde edilen tüm sonuçlar, önerilen teori ile iyi bir ilişki göstermektedir.

**Anahtar Kelimeler:** Sayısal FIR Süzgeç, Kenar-lob Yuvarlanma Oranı, Uzak-son Durduran Bant Zayıflatması, Pencere Tekniği, Kaiser Penceresi, Üstsel Pencere

**I lovingly dedicate this thesis**

**To my beloved father**

**To my beloved mother**

**To my two brothers**

**To my wife**

**To all my friends**

## **ACKNOWLEDGMENTS**

I sincerely acknowledge all the help and support that I was given by Prof. Dr. Hasan K m rc gil whose knowledge, guidance, and effort made this research go on and see the light.

I would like to express my deep gratitude to my mother and father for their support, effort, pain, and patience and to whom I own the success of my life. Special thanks go to my wife Hala and my friends Omar Hayman, Humam Mohammed, Hayder Mohammed, Liwaa Hussein, Anas Qasim, Ahmed Hani, Mohammed AL-Sayed, Sinan Hazem, and Bessam Al-Jewad and to all my friends for their help and support.

# TABLE OF CONTENTS

ABSTRACT .....	iii
ÖZ .....	v
ACKNOWLEDGMENTS.....	vii
LIST OF FIGURES.....	x
LIST OF TABLES .....	xii
1 INTRODUCTION.....	1
2 FIR FILTERS .....	4
2.1 Structures of FIR Systems .....	4
2.1.1 Direct Form.....	4
2.1.2 Cascade Form .....	5
2.1.3 Linear Phase Filters .....	5
2.1.4 Frequency Sampling .....	12
2.2 FIR Filter Design Methods.....	14
2.2.1 FIR Filters Specifications .....	15
2.2.2 FIR Coefficient Calculation Methods.....	17
3 FIR FILTER DESIGN USING EXPONENTIAL WINDOW .....	25
3.1 Spectral Characteristics of Windows.....	25
3.2 Introduction of the Exponential Window .....	27
3.3 FIR Filter Design Using Exponential Window.....	29
4 COMPUTER SIMULATIONS .....	35



4.1 FIR Filter Design by Kaiser Window.....	36
4.2 FIR Filter Design by Cosh Window.....	37
4.3 FIR Filter Design by Exponential Window.....	38
4.4 Performance Comparison of the Filters.....	40
5 CONCLUSIONS.....	43
REFERENCES.....	45
APPENDICES.....	47
Appendix A1: Simulations of FIR Filter Design by Exponential, Kaiser and Cosh Window.....	48
Appendix A2: Performance Comparison of the Filters.....	50

# LIST OF FIGURES

Figure 1: Direct Form Structure .....	4
Figure 2: An FIR Filter Implemented as a Cascade of Second-order Systems.....	5
Figure 3: Direct Form Implementations for Linear Phase Filters. (a) Type I, III (b) Type II, IV.....	6
Figure 4: Unit Impulse Response of Type I FIR Linear Phase Filter .....	8
Figure 5: Unit Impulse Response of Type II FIR of Linear Phase FIR Filter .....	10
Figure 6: Unit Impulse Response of Type III FIR of Linear Phase FIR Filter .....	11
Figure 7: Unit Impulse Response of Type IV FIR of Linear Phase FIR Filter .....	11
Figure 8: Frequency Sampling Filter Structure.....	13
Figure 9: Summary of Design Stages for Digital Filters.....	15
Figure 10: Specification of Magnitude-frequency Response for a Lowpass Filter ...	16
Figure 11: Comparison of the Frequency Response of (a) the window filter and (b) the optimal filter. In (a) the ripples are largest near bandedge; in (b) the ripples have the same peaks (equiripple) in the passband or stopband .....	18
Figure 12: (a) Ideal Frequency Response of a Lowpass Filter. (b) Impulse Response of the Ideal Lowpass Filter.....	20
Figure 13: Effects on the Frequency Response of Truncating the Ideal Impulse Response to (a) 13 coefficients, (b) 25 coefficients and (c) an infinite number of coefficients.....	22
Figure 14: An Illustration of how the Filter Coefficients, $h(nT)$ are Determined by the Window Method.....	23
Figure 15: Amplitude Spectrum and Some Common Spectral Characteristics of a Typical Normalized Window .....	26

Figure 16: The Functions $\exp(x)$ and $\text{Io}(x)$ Characteristics which have Similar Shape .....	28
Figure 17: Proposed Window Spectrum in dB for $\alpha_{cx}= 0, 2,$ and $4$ and $N=51$ .....	29
Figure 18: Amplitude Spectrums of the Filters Designed by the Exponential Window for Various Alpha with $N=127$ .....	30
Figure 19: The Relation between Alpha and the Minimum Stopband Attenuation for Exponential Window with $N=127$ .....	32
Figure 20: The Difference in the Minimum Stopband Attenuation with $N=127$ between the Filters Designed by Exponential and Kaiser Windows .....	33
Figure 21: The Difference between the Designed Filters once when Exponential and Kaiser windows, the term of Comparison is the Maximum Stopband Attenuation with $N=127$ .....	34
Figure 22: Frequency Response of FIR Filter Obtained by Kaiser Window, where $F$ =frequency and $A$ =magnitude .....	36
Figure 23: Frequency Response of FIR Filter Obtained by Cosh Window, where $F$ =frequency and $A$ =magnitude .....	37
Figure 24: Frequency Response of FIR Filter Obtained by Exponential Window, where $F$ =frequency and $A$ =magnitude.....	38
Figure 25: (a) Sinusoidal Input, (b) Outputs of the Filter Obtained by Kaiser, Cosh and Exponential windows .....	40
Figure 26: (a) Sinusoidal Input, (b) Outputs of the Filter Obtained by Kaiser, Cosh and Exponential windows .....	41

## LIST OF TABLES

Table 1: Summary of Ideal Impulse Responses $h_D(n)$ for Standard Frequency Selective Filters .....	21
Table 2: Comparison of FIR Filters Designed by Kaiser, Cosh and Exponential Windows .....	39

# Chapter 1

## INTRODUCTION

A more comprehensive view of the truncation and smoothing operations is in terms of window functions (or windows for short). Windows are normally compared and classified into different types according to their spectral characteristics. Window functions have been widely used in various digital signal processing (DSP) applications such as signal analysis, signal estimation, digital filter design and speech processing [1] [2].

Various windows have been proposed to achieve the desired solutions [3] [4] [2] [5]. Cosine hyperbolic function is one of them [6]. The idea of this window is based on the Kaiser window, but it has an advantage since there is no expanding in the power series in the time domain representation. This window gives a better ripple ratio for wider main lobe width and larger side lobe roll-off ratio along with the ultraspherical comparison. When its function is merged with the Hamming window, it produces a better performance in terms of the ripple ratio, better than a same margin of a Kaiser and Hamming windows. Another method to design ultraspherical window functions in order to reach prescribed spectral characteristics can be found in [4]. This method is made of combining various techniques basically to measure the ultraspherical window, independent parameters which are ripple ratio and main-lobe width or null-to-null width along with a user-defined side-lobe pattern can also be reached. A simple comparison has been made between the ultraspherical

and Kaiser windows and the result of this comparison showed that there is a difference in the performance which depends on the required specifications.

It is well known that the Kaiser window is a flexible one which is used in applications such as digital filter design and spectrum analysis [6] [2]. The advantage of using the Kaiser window is that it accomplishes a good approximation to the discrete prolate spheroidal functions whose mainlobe has a maximum concentration of energy. There are two main independent parameters in the Kaiser window: the first one is the window length ( $N$ ) and the second one is the shape parameter alpha ( $\alpha$ ). For different applications, it is possible to control the mainlobe width, ripple ratio and sidelobe roll off ratio by changing these two parameters.

In some applications such as beamforming [7], digital filter design and speech processing [4], the sidelobe roll off ratio is a significant parameter. A beamforming application is required to have a large sidelobe roll off ratio for ignoring the far end interference [4]. On the other hand, the sidelobe roll off ratio can reduce the far end attenuation for stopband energy in filter a design application. Furthermore, it can reduce the energy leak from one band to another in speech processing applications.

There are many useful adjustable windows for instance Saramaki [5] and Dolph-Chebyshev [3]. In fact, they are special form of Ultrapherical window [7]. However, the sibelobe roll off characteristics of the Kaiser window is better than the last mentioned two windows. In some applications, it could be quite reasonable to obtain a window that could provide higher sidelobe roll off characteristics than what Kaiser window provides.

It has been noted that the window based on exponential function offers a higher sidelobe roll off ratio compared to the Kaiser window [8]. In this thesis, the idea of exponential window has been explored for designing the digital nonrecursive finite impulse response (FIR) filters. It is shown that the FIR filter designed with the help of exponential window provides better far-end stopband attenuation against filters designed by well-known windows in literature.

The thesis is organized as follows: chapter two gives information about the structure of FIR filters and the design methods such as the optimal method, frequency sampling method and window method. In chapter three, FIR filter design using exponential window is explained, and in chapter four, the computer simulations obtained from FIR filters which are designed by Kaiser, Cosh and Exponential windows are presented and discussed. Finally, chapter five addresses the conclusions and the future work.

## Chapter 2

### FIR FILTERS

#### 2.1 Structures of FIR Systems

A basic FIR filter is of a polynomial system function in  $z^{-1}$  as shown below

$$H(z) = \sum_{n=0}^N h(n)z^{-n} \quad (2-1)$$

where  $H(z)$  is the transfer function of the FIR filter,  $h(n)$  is the impulse response,  $z^{-1}$  represents a delay of one sample time,  $n$  represents discrete time and  $N$  represents the filter length (number of coefficients). For an input  $x(n)$ , the output is determined by

$$y(n) = \sum_{k=0}^N h(k)x(n-k) \quad (2-2)$$

Equation (2-2) is known as the convolution sum equation. Calculation of this sum needs  $(N + 1)$  multiplications and  $N$  additions for every  $n$  value.

##### 2.1.1 Direct Form

Figure 1 shows the realization of equation (2-2) by using a tapped delay line method.

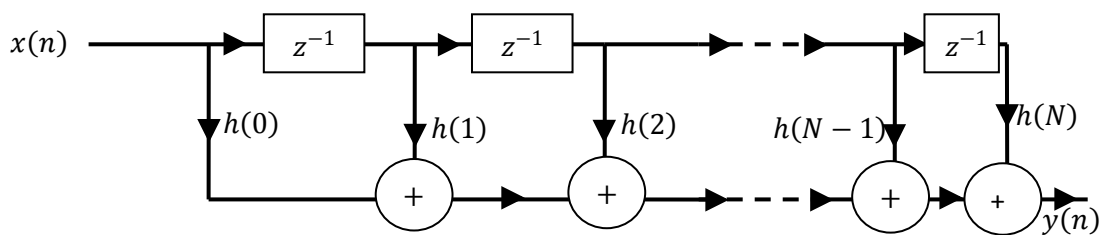


Figure 1: Direct Form Structure



The computation of each output sample,  $y(n)$ , requires  $N + 1$  multiplications,  $N$  additions, and  $N$  delays. But, in the case of any similarity in the unit sample response, it is possible to decrease the multiplications number.

### 2.1.2 Cascade Form

For a basic FIR filter, the transfer function could be factored into first-order factors,

$$H(z) = \sum_{n=0}^N h(n)z^{-n} = A \prod_{k=1}^N (1 - \alpha_k z^{-1}) \quad (2-3)$$

where  $\alpha_k$  for  $k = 1, \dots, N$  are the zeros of  $H(z)$ . The complex roots of  $H(z)$  happen in complex conjugated pairs if  $h(n)$  is real and these conjugated pairs can be combined to form second-order factors with real coefficients,

$$H(z) = A \prod_{k=1}^{N_s} [1 + b_k(1)z^{-1} + b_k(2)z^{-2}] \quad (2-4)$$

$H(z)$ , in this form, may be applied as a cascade of second-order FIR filters as illustrated in Fig. 2.

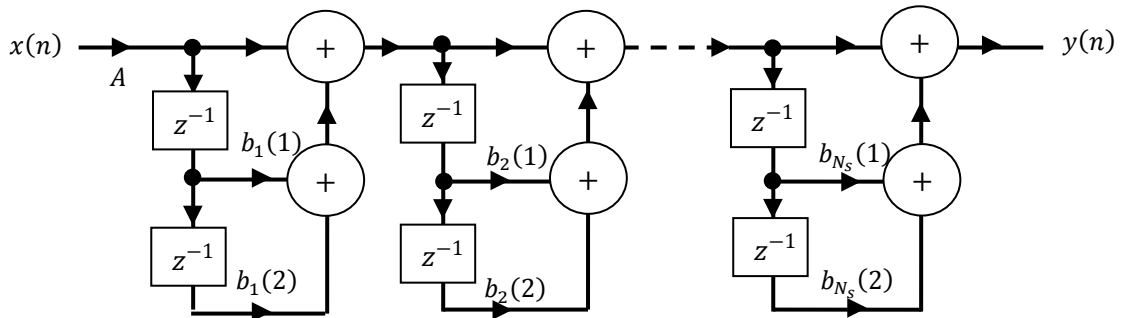


Figure 2: An FIR Filter Implemented as a Cascade of Second-order Systems

### 2.1.3 Linear Phase Filters

Filters with linear phase have a unit sample response that is either symmetric,

$$h(n) = h(N - n) \quad (2-5)$$

or anti-symmetric (see sec. 2.1.3.1)

$$h(n) = -h(N - n) \quad (2-6)$$

This symmetric could be exploited to shorten the network structure and make it easier to use. An example for it, if  $N$  is even and  $h(n)$  is symmetric (type I filter),

$$y(n) = \sum_{k=0}^N h(k)x(n-k) = \sum_{k=0}^{\frac{N}{2}-1} h(k)[x(n-k) + x(n-N+k)] + h\left(\frac{N}{2}\right)x\left(n-\frac{N}{2}\right) \quad (2-7)$$

Consequently, making the sums  $[x(n-k) + x(n-N+k)]$  prior to multiplying by  $h(k)$  decreases the multiplications numbers. The out coming structure is in Figure 3 (a). On the other hand, if  $N$  is odd and  $h(n)$  is symmetric (type II filter), the resulting structure is as in Figure 3 (b). There are similar anti-symmetric structures (types III and IV) linear phase filters.

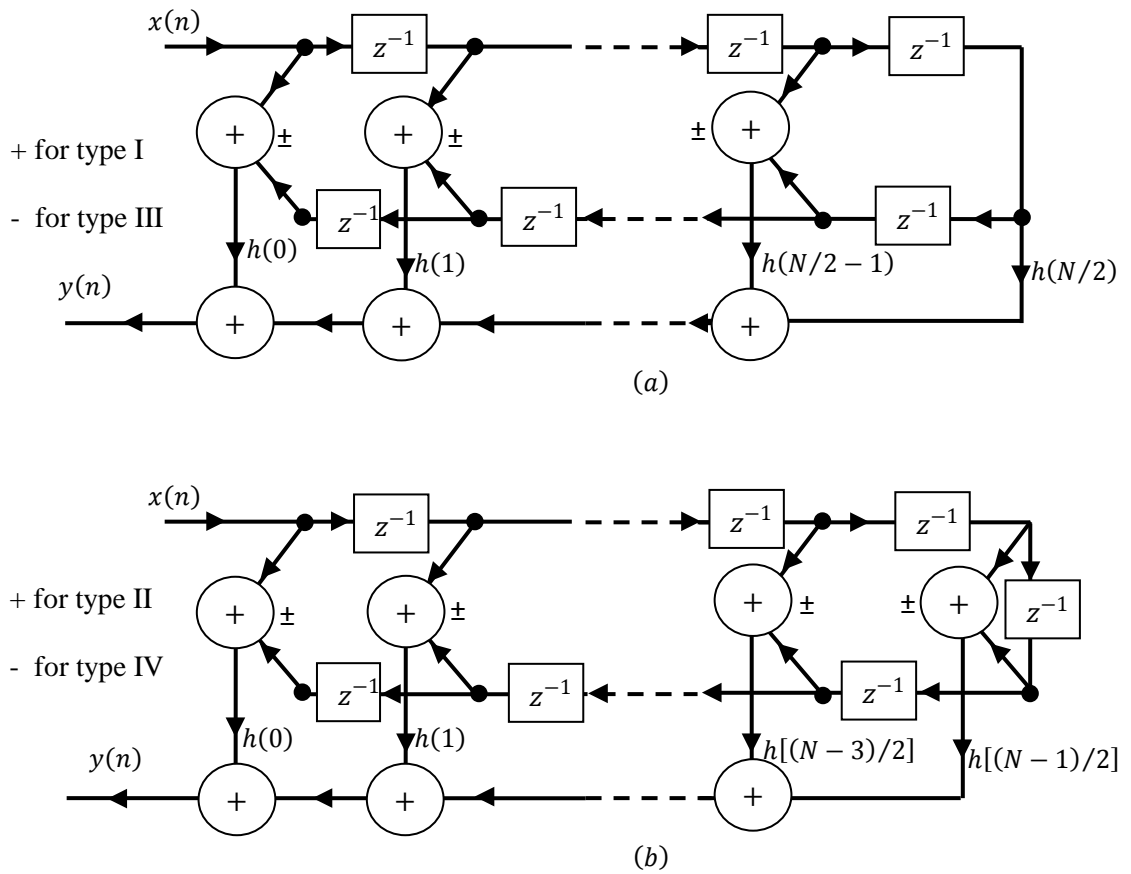


Figure 3: Direct Form Implementations for Linear Phase Filters. (a) Type I, III (b) Type II, IV

### 2.1.3.1 Types of Linear Phase FIR Filters

Let us consider the unique kinds of FIR filters where the coefficients  $h(n)$  of the transfer function

$$H(z^{-1}) = \sum_{n=0}^N h(n)z^{-n} \quad (2-8)$$

are supposed to be symmetric or anti-symmetric. Since the organization of the polynomial in both of these two kinds can be either odd or even, there are four kinds of filters with diverse properties, which will be explained next [9].

**Type I.** Coefficients are symmetric [ $h(n) = h(N - n)$ ], and the order  $N$  is even.

In general, coefficient can be expressed in some other forms. Let us assume that the order is even. The transfer function in equation (2-8) can be expanded as:

$$\begin{aligned} H(z^{-1}) &= \sum_{n=0}^N h(n)z^{-n} \\ &= h(0) + h(1)z^{-1} + h(2)z^{-2} + \dots + h(N-1)z^{-N+1} + h(N)z^{-N} \end{aligned} \quad (2-9)$$

For type I filter with  $N$  order, as shown in Fig. 4, it is noted that  $h(0) = h(N)$ ,  $h(1) = h(N-1)$ , ...,  $h(n) = h(N-n)$ . Applying these relationships in the equation above, we get

$$H(z^{-1}) = h(0)[1 + z^{-N}] + h(1)[z^{-1} + z^{-N+1}] + \dots + h\left(\frac{N}{2}\right)z^{-\frac{N}{2}} \quad (2-10)$$

This can also be shown as in the following form

$$\begin{aligned} H(z^{-1}) &= z^{-\frac{N}{2}} \left\{ h(0) \left[ z^{\frac{N}{2}} + z^{-\frac{N}{2}} \right] + h(1) \left[ z^{-1+\frac{N}{2}} + z^{-N+1+\frac{N}{2}} \right] + \dots \right. \\ &\quad \left. + h\left(\frac{N}{2}\right) \right\} \end{aligned} \quad (2-11)$$

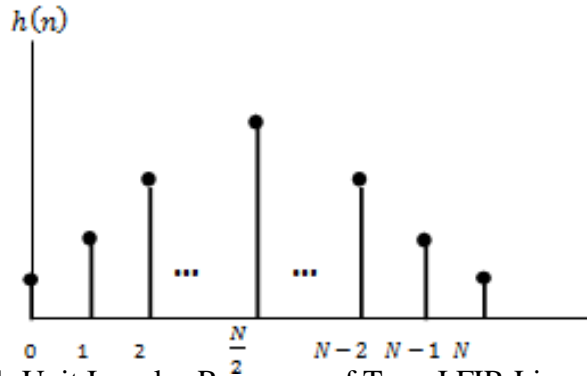


Figure 4: Unit Impulse Response of Type I FIR Linear Phase Filter

The frequency response of equation (2-11) is given by

$$H(e^{-j\omega}) = e^{j\theta\omega} \{H_R(\omega)\} \quad (2-12)$$

In this formula, the term  $H_R(\omega)$  is a real-valued function; however it can be negative or positive at any specific frequency, therefore while transforming from a positive value to a negative one, the angle of the phase changes by  $\pi$  radians ( $180^\circ$ ). The angle of the phase  $\theta(\omega) = -3\omega$  is a linear function of  $\omega$ , and the group delay  $\tau$  is the same as three samples. Remember that the group delay is three samples on the normalized frequency basis, but the real the group delay is  $3T$  seconds, where  $T$  denotes the sampling period. In general,  $H(e^{j\omega})$  can be expressed in some other forms

$$\begin{aligned} H(e^{j\omega}) &= \sum_{n=0}^N h(n)e^{-jn\omega} \\ &= h(0) + h(1)e^{-j\omega} + h(2)e^{-2j\omega} + \dots + h(N-1)e^{-j(N\omega)} \\ &= e^{-j[(N/2)\omega]} \left\{ 2h(0) \cos\left(\frac{N\omega}{2}\right) + 2h(1) \cos\left(\left(\frac{N}{2}-1\right)\omega\right) + 2h(2) \cos\left(\left(\frac{N}{2}-2\right)\omega\right) + \dots \right. \\ &\quad \left. + h\left(\frac{N}{2}\right) \right\} \end{aligned} \quad (2-13)$$

and now in a more compact form:

$$H(e^{j\omega}) = e^{-j[(N/2)\omega]} \left\{ h\left(\frac{N}{2}\right) + 2 \sum_{n=1}^{N/2} h\left[\frac{N}{2} - n\right] \cos(n\omega) \right\} = e^{j\omega} \{H_R(\omega)\} \quad (2-14)$$

The whole the group delay is constant  $\tau = N/2$  in the general case, for a type I FIR filter.

**Type II.** Coefficients are symmetric [ $h(n) = h(N - n)$ ], and the order  $N$  is odd.

Now, if we consider symmetric coefficients with  $N$  odd, we obtain the impulse response shown in Figure 5.

$$H(z^{-1}) = \sum_{n=0}^N h(n)z^{-n} = h(0) + h(1)z^{-1} + h(2)z^{-2} + \dots + h(N)z^{-N} \quad (2-15)$$

and due to symmetry

$$h(0) = h(N), h(1) = h(N - 1), h(2) = h(N - 2), \dots, h(n) = h(N - n) \quad (2-16)$$

Now, if we consider symmetric coefficients with  $N$  odd, the impulse response is shown in Figure 5.

The frequency response is in the type II filter for general case can be written as

$$\left. \begin{aligned} H(e^{-j\omega}) &= \sum_{n=0}^N h(n)e^{-jn\omega} = e^{j\theta(\omega)} \{H_R(\omega)\} \\ &= e^{-j\left(\frac{N}{2}\omega\right)} \left\{ \sum_{n=1}^{(N+1)/2} 2h\left[\frac{N+1}{2} - n\right] \cos\left(\left(n - \frac{1}{2}\right)\omega\right) \right\} \end{aligned} \right\} \quad (2-17)$$

which demonstrates a linear phase  $\theta(\omega) = -[(N/2)\omega]$  and a constant group delay  $\tau = N/2$  samples.

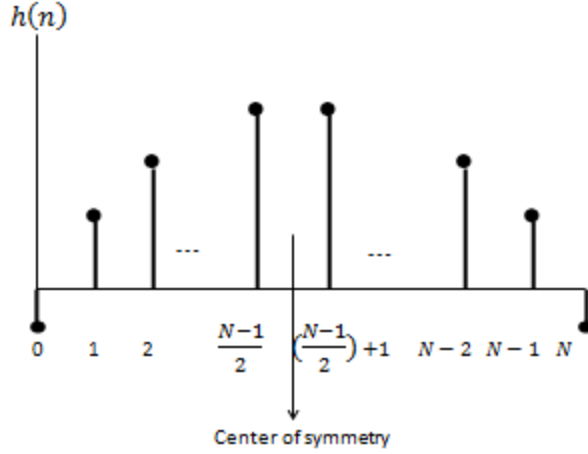


Figure 5: Unit Impulse Response of Type II FIR of Linear Phase FIR Filter

**Type III.** The coefficients are anti-symmetric [ $h(n) = -h(N - n)$ ], and the order  $N$  is even. Figure 6 shows that  $h(0) = -h(N)$ ,  $h(1) = -h(N - 1)$ ,  $h(2) = -h(N - 2)$  and  $h(N/2) = 0$  to preserve anti-symmetry for these samples:

$$H(z^{-1}) = h(0)[1 - z^{-N}] + h(1)[z^{-1} - z^{-N+1}] + \dots + h\left(\frac{N}{2}\right)z^{-\frac{N}{2}} \quad (2-18)$$

This can also be shown as in the following form

$$H(z^{-1}) = z^{-\frac{N}{2}} \left\{ h(0) \left[ z^{\frac{N}{2}} - z^{-\frac{N}{2}} \right] + h(1) \left[ z^{-1+\frac{N}{2}} - z^{-N+1+\frac{N}{2}} \right] + \dots + h\left(\frac{N}{2}\right) \right\} \quad (2-19)$$

Here if we place  $z = e^{j\omega}$ , and  $e^{j\omega} - e^{-j\omega} = 2j \sin(\omega) = 2e^{j(\pi/2)} \sin(\omega)$ , we get the frequency response in the general case as

$$H(e^{-j\omega}) = e^{-j[(N\omega - \pi)/2]} \left\{ 2 \sum_{n=1}^{N/2} h \left[ \frac{N}{2} - n \right] \sin(n\omega) \right\} \quad (2-20)$$

and it has a linear phase  $\theta(\omega) = -[(N\omega - \pi)/2]$  and the group delay  $\tau = N/2$  samples.

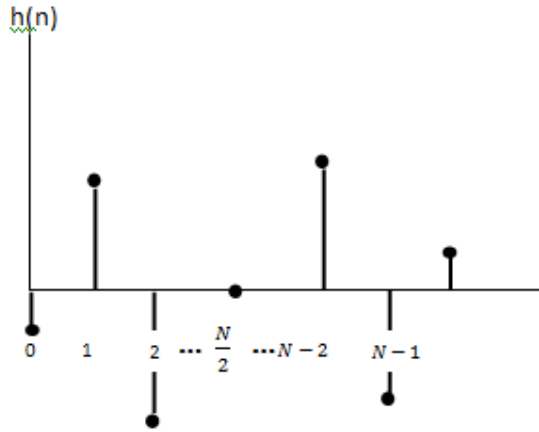


Figure 6: Unit Impulse Response of Type III FIR of Linear Phase FIR Filter

**Type IV.** Coefficients are anti-symmetric [ $h(n) = -h(N - n)$ ], and the order  $N$  is odd. As in Figure7, in which  $h(0) = -h(N)$ ,  $h(1) = -h(N - 1)$ ,  $h(2) = -h(N - 2)$ , ... ,  $h(n) = h(N - n)$ . Its transfer function can be written:

$$H(z^{-1}) = h(0)[1 - z^{-N}] + h(1)[z^{-1} - z^{-N+1}] + \dots + h\left(\frac{N-1}{2}\right)z^{-\frac{N-1}{2}} \quad (2-21)$$

The frequency response of the transfer function of the type IV linear phase filter is usually given by

$$H(e^{-j\omega}) = e^{-j[(N\omega-\pi)/2]} \left\{ 2 \sum_{n=1}^{(N+1)/2} h \left[ \frac{N+1}{2} - n \right] \sin \left( \left( n - \frac{1}{2} \right) \omega \right) \right\} \quad (2-22)$$

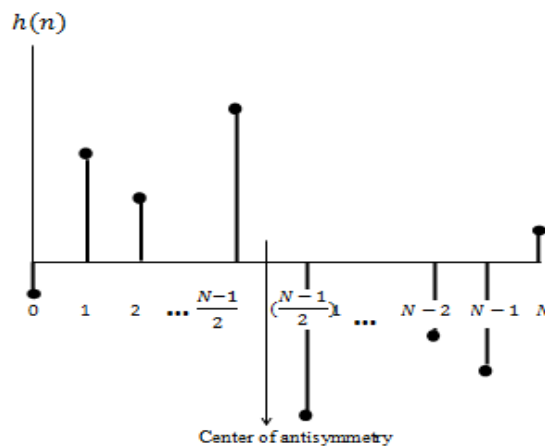


Figure 7: Unit Impulse Response of Type IV FIR of Linear Phase FIR Filter

### 2.1.4 Frequency Sampling

A filter is parameterized after the implementation of frequency sampling structure in terms of its discrete Fourier transform (DFT) coefficients. Particularly, if  $H(k)$  is the  $N$  – point DFT of an FIR filter with  $h(n) = 0$  for  $0 < n > N$ , then the impulse response of the filter is

$$h(n) = \frac{1}{N} \sum_{k=0}^{N-1} H(k) e^{j2\pi nk/N} \quad (2-23)$$

The transfer function can be written as:

$$\begin{aligned} H(z) &= \sum_{n=0}^{N-1} h(n) z^{-n} = \sum_{n=0}^{N-1} \left[ \frac{1}{N} \sum_{k=0}^{N-1} H(k) e^{j2\pi nk/N} \right] z^{-n} \\ &= \frac{1}{N} \sum_{k=0}^{N-1} H(k) \sum_{n=0}^{N-1} e^{j2\pi nk/N} z^{-n} \end{aligned} \quad (2-24)$$

Calculating the sum over  $n$  gives

$$H(z) = \frac{1}{N} (1 - z^{-N}) \sum_{k=0}^{N-1} \frac{H(k)}{1 - e^{j2\pi k/N} z^{-1}} \quad (2-25)$$

which corresponds to an FIR filter cascade  $\frac{1}{N} (1 - z^{-N})$  with one-pole parallel network filters:

$$H(z) = \frac{H(k)}{1 - e^{j2\pi k/N} z^{-1}} \quad (2-26)$$

For a filter with narrowband that has the majority of its DFT coefficients equal to zero, the structure of the frequency sampling shall be an efficient implementation.

The structure of the frequency sampling is given in Figure 8. If  $h(n)$  is real,  $H(k) = H^*(N - k)$ , the structure could be simplified. An example for it, if  $N$  is even, [10]

$$H(z) = \frac{1}{N} (1 - z^{-N}) \left[ \frac{H(0)}{1 - z^{-1}} + \frac{H(N/2)}{1 + z^{-1}} + \sum_{k=1}^{N/2-1} \frac{A(k) - B(k)z^{-1}}{1 - 2 \cos(2\pi k/N) z^{-1} + z^{-2}} \right] \quad (2-27)$$



where

$$A(k) = H(k) + H(N - k) \quad (2-28)$$

$$B(k) = H(k)e^{-j2\pi k/N} + H(N - k)e^{j2\pi k/N} \quad (2-29)$$

On the other hand, when  $N$  is odd similar simplification results can be obtained.

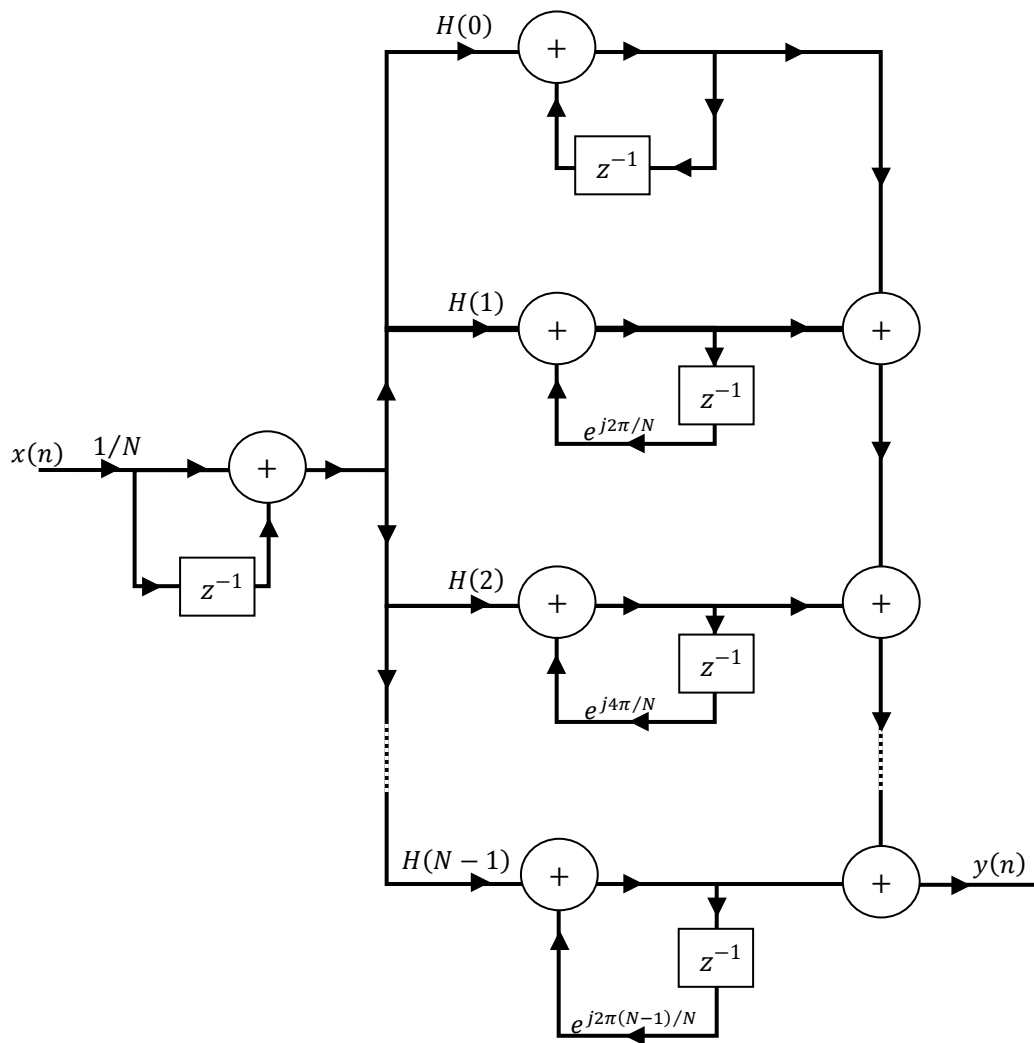


Figure 8: Frequency Sampling Filter Structure

## 2.2 FIR Filter Design Methods

There are five steps in the process of designing a digital filter:

(i) Specifying the type of filter. For example, lowpass filter the preferred amplitude and/or phase responses and the acceptable tolerances, the sampling frequency, and the length of words in the input data.

(ii) Determining the coefficients of a transfer function,  $H(z)$ , that satisfy the specifications given in (i). There are several factors that influence the choice of the method of coefficient calculation. The critical requirements in step (i) are the most important of these factors.

(iii) Converting the transfer function obtained in (ii) into a suitable filter network or structure, which is known as realization.

(iv) Analysing the effects of finite word length. Here, the effect of quantizing the filter coefficients and the input data as well as the effect of carrying out the filtering operation are analysed by using fixed word lengths on the filter performance.

(v) Producing the software code and/or hardware and performing the actual filtering.

These five interrelated steps are summarized in Fig.9.

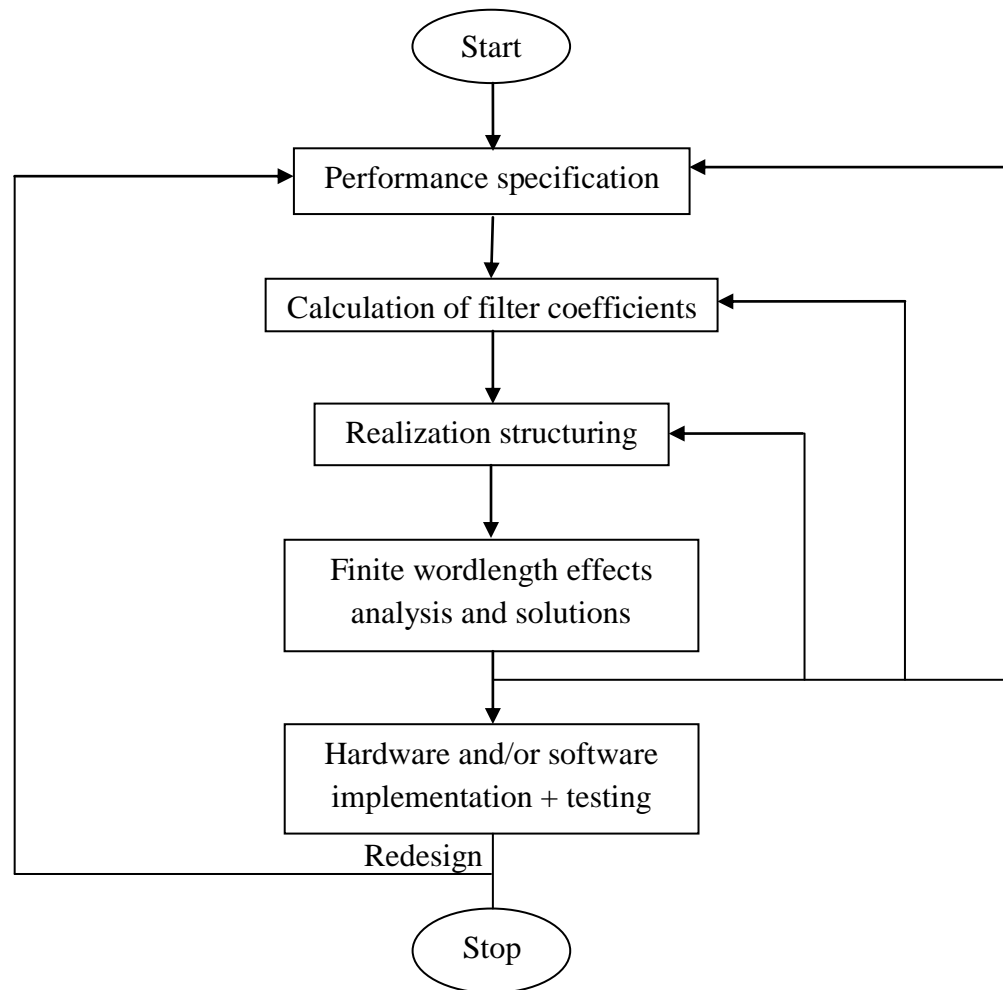


Figure 9: Summary of Design Stages for Digital Filters

### 2.2.1 FIR Filters Specifications

For the phase response, what is needed is to state whether positive symmetry or negative symmetry is required (assuming linear phase). The amplitude-frequency response of an FIR filter is usually determined by a tolerance scheme. Such a scheme for the low pass filter is shown in Figure 10. A similar scheme can be used for other frequency selective filters. Referring to the figure, the following parameters are of interest:

$\delta_p$  peak passband deviation (or ripples)

$\delta_s$  stopband deviation

$f_p$  passband edge frequency

$f_s$  stopband edge frequency

$F_s$  sampling frequency

$\Delta F$  transition band

Practically, it is more suitable to express  $\delta_p$  and  $\delta_s$  in decibels (dB) as shown in the figure. The transition width of the filter is given by the difference between  $f_s$  and  $f_p$ . The filter length is another important parameter. The number of filter coefficients is defined by a given  $N$ . In most cases, these parameters completely define the frequency response of the FIR filter [11].

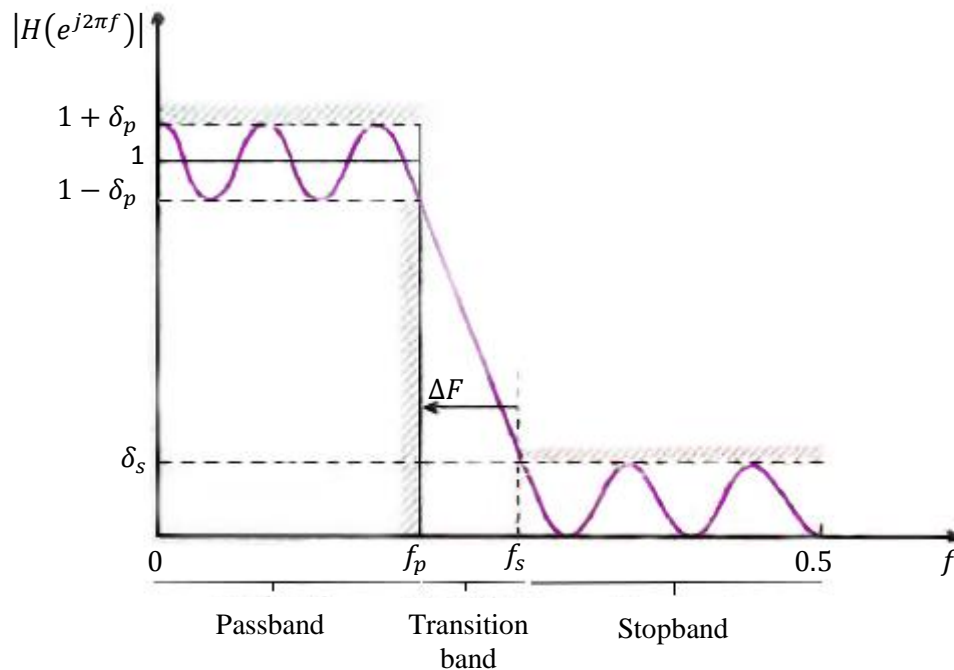


Figure 10: Specification of Magnitude-frequency Response for a Lowpass Filter

The passband deviation in dB is defined as:

$$20\log(1 + \delta_p) \tag{2-30}$$

The stopband deviation in dB is defined as:

$$-20\log(\delta_s) \tag{2-31}$$

Other specifications include the maximum accepted number of filter coefficients (this may be determined by the particular application, such as the speed of operation). It is difficult to select one or more of the parameters above and so trial and error may help to deduce that.

### 2.2.2 FIR Coefficient Calculation Methods

The following equations characterize the FIR filter:

$$y(n) = \sum_{k=0}^{N-1} h(k)x(n-k) \tag{2-32}$$

$$H(z) = \sum_{n=0}^{N-1} h(n)z^{-n} \tag{2-33}$$

The aim of most FIR coefficient calculation (or approximation) methods is to get values of  $h(n)$  in a way that the resulting filter meets the design specifications such as amplitude-frequency response and throughput requirements. There are several methods for obtaining  $h(n)$ . However, the optimal, frequency sampling and window methods are the most commonly used. All three methods lead to linear phase FIR filters.

#### 2.2.2.1 The Optimal Method

The optimal (in the Chebyshev sense) method of calculating FIR filter coefficients is very easy to apply because of the existence of a design program, and very powerful and flexible as well. This method has become the first choice in many FIR applications for the above mentioned reasons and because it yields excellent filters.

In the window method, the problem of finding a suitable approximation to a desired or ideal frequency response is inherent in the process of calculating suitable filter

coefficients. The peak ripple of filters designed by the window method occurs near the band edges, and decreases away from the band edges (Figure 11 (a)).

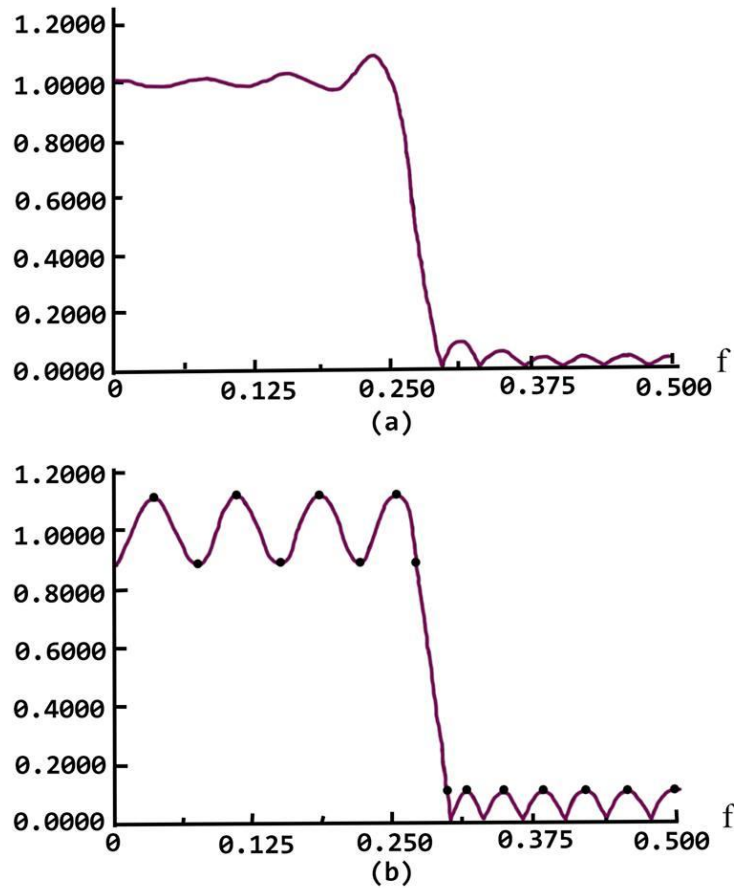


Figure 11: Comparison of the Frequency Response of (a) the window filter and (b) the optimal filter. In (a) the ripples are largest near bandedge; in (b) the ripples have the same peaks (equiripple) in the passband or stopband

If the ripples were distributed equally over the passband and stopband as in Figure 11 (b), we can achieve a better approximation of the desired frequency response.

### 2.2.2.2 Frequency Sampling Method

The frequency sampling method helps in designing nonrecursive FIR filters for both standard frequency selective filters (lowpass, highpass, bandpass filters) and filters with arbitrary frequency response. A unique attraction of the frequency sampling method is that it also allows recursive implementation of FIR filters, which leads to

computationally well-organized filters. With some limits, recursive FIR filters whose coefficients are simple integers may be designed, which is attractive when only primitive arithmetic operations are possible, as in systems implemented with standard microprocessors.

### 2.2.2.3 Window Method:

In this method, the frequency response of a filter  $H_D(\omega)$ , and the corresponding impulse response,  $h_D(n)$ , are related by the inverse Fourier transform below:

$$h_D(n) = \frac{1}{2\pi} \int_{-\pi}^{\pi} H_D(\omega) e^{j\omega n} d\omega \quad (2-34)$$

To distinguish between the ideal and practical impulse responses, the subscript D is used. This distinction is clearly needed. If  $H_D(\omega)$  is known,  $h_D(n)$  can be obtained by evaluating the inverse Fourier transform of equation (2-34). To illustrate that, presume that we need to design a lowpass filter. We can start with the ideal lowpass response revealed in Figure 12(a) where  $\omega_c$  is the cutoff frequency and the frequency scale is normalized  $T = 1$ . By letting the response go from  $-\omega_c$  to  $\omega_c$ , the integration operation is simplified. Thus, the impulse response is given by:

$$\left. \begin{aligned} h_D(n) &= \frac{1}{2\pi} \int_{-\pi}^{\pi} 1 \times e^{j\omega n} d\omega = \frac{1}{2\pi} \int_{-\omega_c}^{\omega_c} e^{j\omega n} d\omega \\ &= \frac{2f_c \sin(n\omega_c)}{(n\omega_c)}, \quad n \neq 0, -\infty \leq n \leq \infty \\ &= 2f_c, \quad n = 0 \end{aligned} \right\} \quad (2-35)$$

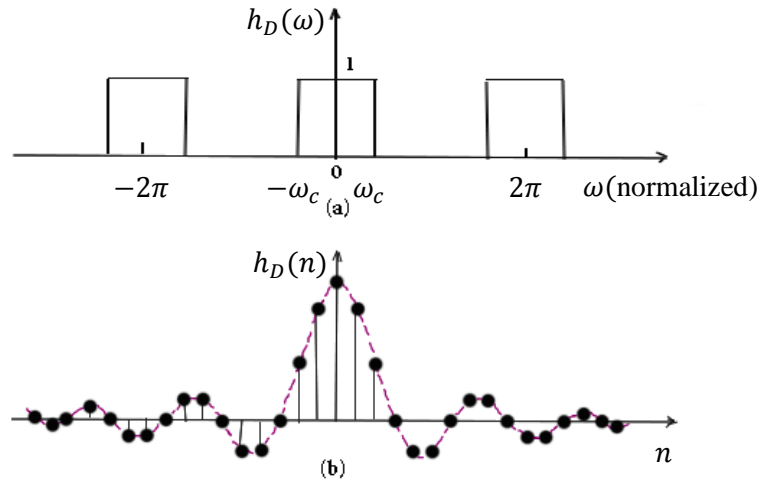


Figure 12: (a) Ideal Frequency Response of a Lowpass Filter. (b) Impulse Response of the Ideal Lowpass Filter

The low pass case of equation (2-35) gives the impulse responses for the ideal highpass, bandpass and bandstop filters as summarized in Table 1. The impulse response for the low pass filter is shown in Figure 12(b) from which it is noted that  $h_D(n)$  is symmetrical about  $n = 0$  (that is  $h_D(n) = h_D(-n)$ ), so that the filter will have a linear (in this case zero) phase response. Several practical problems with this simple approach are clear. The most important of these is that, although  $h_D(n)$  decreases as we move away from  $n = 0$ , theoretically, it carries on to  $n = \pm\infty$ , thus, the resulting filter is not an FIR.

An obvious solution is to truncate the ideal impulse response by setting  $h_D(n) = 0$  for  $n$  greater than  $M$ . However, this gives undesirable ripples and overshoots—the so-called Gibbs' phenomenon. The effects of discarding coefficients on the filter response are shown in Figure 13. The more coefficients that are retained, the closer the filter spectrum is to the ideal response (Figures 13(b) and 13(c)). Direct



truncation of  $h_D(n)$  as described above is equivalent to multiplying the ideal impulse response by a rectangular window of the form

$$w(n) = 1, \quad |n| = 0, 1, \dots, (M - 1)/2$$

$$0, \quad \text{else where} \quad (2-36)$$

Table 1: Summary of Ideal Impulse Responses  $h_D(n)$  for Standard Frequency Selective Filters

Filter type	$h_D(n), n \neq 0$	$h_D(0)$
Lowpass	$2f_c \frac{\sin(n\omega_c)}{n\omega_c}$	$2f_c$
Highpass	$-2f_c \frac{\sin(n\omega_c)}{n\omega_c}$	$1 - 2f_c$
Bandpass	$2f_2 \frac{\sin(n\omega_2)}{n\omega_2} - 2f_1 \frac{\sin(n\omega_1)}{n\omega_1}$	$2(f_2 - f_1)$
Bandstop	$2f_1 \frac{\sin(n\omega_1)}{n\omega_1} - 2f_2 \frac{\sin(n\omega_2)}{n\omega_2}$	$1 - 2(f_2 - f_1)$

$f_c, f_1$  and  $f_2$  are the normalized passband or stopband edge frequencies; N is the length of filter.

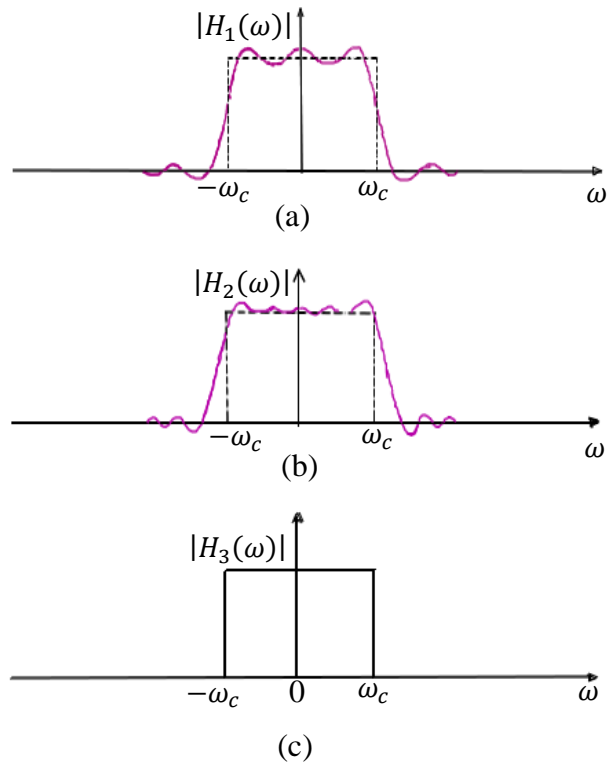


Figure 13: Effects on the Frequency Response of Truncating the Ideal Impulse Response to (a) 13 coefficients, (b) 25 coefficients and (c) an infinite number of coefficients

In the frequency domain this is equivalent to convolving  $H_D(\omega)$  and  $W(\omega)$ , where  $W(\omega)$  is the Fourier transform of  $w(n)$ . Truncation of  $h_D(n)$  leads to the overshoots and ripples in the frequency response because  $W(\omega)$  has the classic  $(\sin x)/x$  shape. A practical approach is to multiply the ideal impulse response,  $h_D(n)$ , by an appropriate window function  $w(n)$ , whose duration is finite so that the resulting impulse response decays smoothly towards zero. The process is shown in Figure 14. The ideal frequency response and the corresponding ideal impulse response are shown in Figure 14(a). Whereas, Figure 14(b) illustrates a finite duration window function and its spectrum  $h(nT)$  which is obtained by multiplying  $h_D(nT)$  by  $w(nT)$  is shown in Figure 14(c).

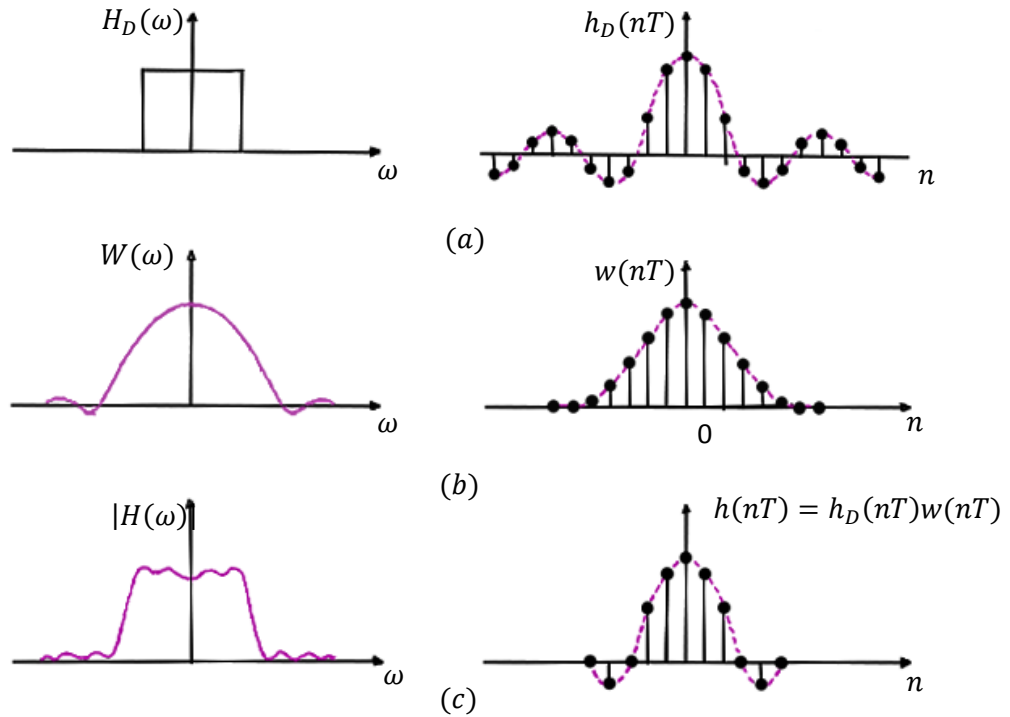


Figure 14: An Illustration of how the Filter Coefficients,  $h(nT)$  are Determined by the Window Method

The corresponding frequency response shows that the ripples and overshoots, characteristic of direct truncation, are much reduced. However, the transition width is wider than for the rectangular case. The transition width of the filter is limited by the width of the main lobe of the window. Ripples are produced by the side lobes in both passband and stopband [11]. Some common window functions are:

i) Hamming window is the most important one of the many common window functions can be defined as:

$$w(n) = \begin{cases} 0.54 + 0.46 \cos(2\pi n/N) & \begin{cases} -(N-2)/2 \leq n \leq (N-1)/2 & (N \text{ odd}) \\ -N/2 \leq n \leq N/2 & (N \text{ even}) \end{cases} \\ 0 & \text{elsewhere} \end{cases} \quad (2-37)$$

ii) Hanning window is defined as:

$$w(n) = \begin{cases} 0.5 + 0.5 \cos(2\pi n/N) & \begin{cases} -(N-2)/2 \leq n \leq (N-1)/2 & (N \text{ odd}) \\ -N/2 \leq n \leq N/2 & (N \text{ even}) \end{cases} \\ 0 & \text{elsewhere} \end{cases} \quad (2-38)$$

iii) Blackman window is defined as:

$$w(n) = \begin{cases} 0.42 + 0.5 \cos(2\pi n/N - 1) + (4\pi n/N - 1) & \begin{cases} -(N-2)/2 \leq n \leq (N-1)/2 & (N \text{ odd}) \\ -N/2 \leq n \leq N/2 & (N \text{ even}) \end{cases} \\ 0 & \text{elsewhere} \end{cases} \quad (2-39)$$

iv) Kaiser window is defined as:

$$w_k(n) = \begin{cases} \frac{I_0(\alpha_k \sqrt{1 - (\frac{2n}{N-1})^2})}{I_0(\alpha_k)} & |n| \leq \frac{N-1}{2} \\ 0 & \text{otherwise} \end{cases} \quad (2-40)$$

where  $\alpha_k$  is the adjustable parameter and  $I_0(x)$  is the modified Bessel function of the first kind of order zero which is described by the power series expansion as

$$I_0(x) = 1 + \sum_{k=1}^{\infty} \left[ \frac{1}{k!} \left( \frac{x}{2} \right)^k \right]^2 \quad (2-41)$$

v) Cosh window is defined as:

$$w_c(n) = \begin{cases} \frac{\cosh(\alpha_{ch} \sqrt{1 - (\frac{2n}{N-1})^2})}{\cosh(\alpha_{ch})} & |n| \leq \frac{N-1}{2} \\ 0 & \text{otherwise} \end{cases} \quad (2-42)$$

## Chapter 3

### FIR FILTER DESIGN USING EXPONENTIAL WINDOW

#### 3.1 Spectral Characteristics of Windows

A window function  $w(nT)$  having a length of  $N$  is a time-domain function which is nonzero for  $n \leq |(N - 1)/2|$  and zero for other values of  $n$ . The frequency spectrum of  $w(nT)$  can be defined as

$$W(e^{j\omega t}) = e^{-j\theta(\omega)}W_0(e^{j\omega t}) \quad (3-1)$$

where  $W_0(e^{j\omega t})$  stands for the amplitude function. The amplitude and phase spectrums of a window function are defined as  $A(\omega) = |W_0(e^{j\omega t})|$  and  $\theta(\omega)$ , respectively. The amplitude spectrum in the normalized form is given by  $|W_0(e^{j\omega t})|/W_0(e^0)$ .

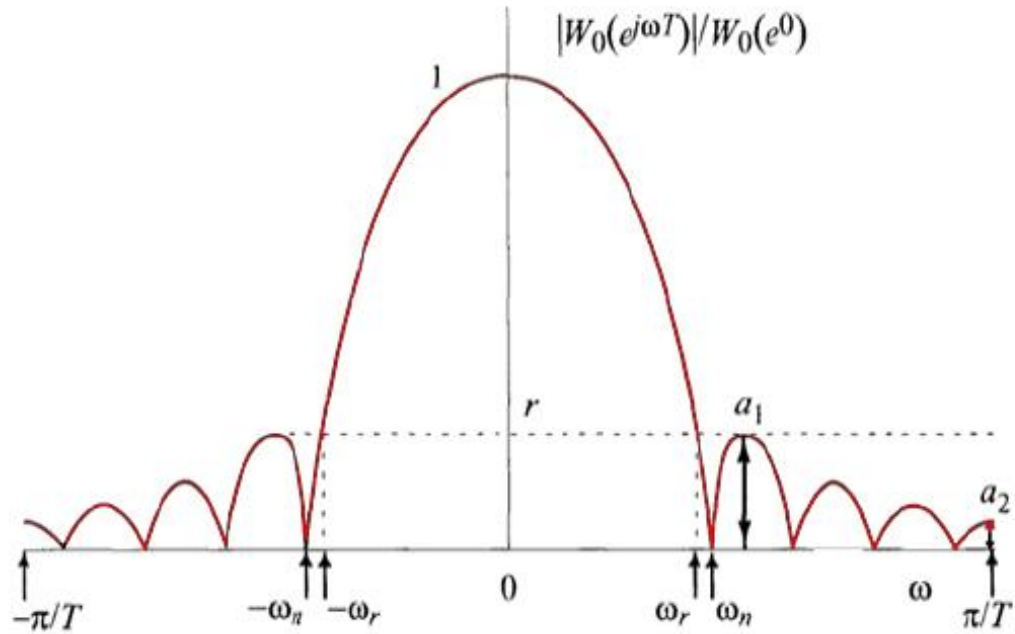


Figure 15: Amplitude Spectrum and Some Common Spectral Characteristics of a Typical Normalized Window

Typical normalized amplitude spectrum of a window together with some spectral characteristics is shown in Fig. 15. One of the most important variables of the window is the ripple ratio (see the Fig. 15) which is defined as in the following equation:

$$r = \frac{\text{maximum sidelobe amplitude}}{\text{main lobe amplitude}} \quad (3-2)$$

Since the ripple ratio is a small quantity less than unity, it is more suitable to consider its larger amounts by using the reciprocal of  $r$  in decibels (dB) as:

$$R = 20 \log_{10} \frac{1}{r} \quad (3-3)$$

where  $R$  represents the minimum side-lobe attenuation (or equivalently minimum stopband attenuation) with respect to the main lobe. In addition, the second parameter that describes the side-lobe pattern of a window is the side-lobe roll-off ratio whose definition is given by:

$$S = \frac{a_1}{a_2} \quad (3-4)$$

where  $a_1$  represents the amplitude of the nearest side lobe,  $a_2$  represents the amplitude of the furthest side lobe (see Fig. 15). The side-lobe roll-off ratio,  $S$ , can be obtained from its dB domain as follows

$$S = 10^{S/20} \quad (3-5)$$

In order to have a logical meaning of the side-lobe roll-off ratio, the side-lobe pattern envelope should be increased or decreased monotonically. Also, the side-lobe roll-off ratio gives an explanation of the energy distribution over the side lobes that could be considered important, when prior knowledge of the location of an interfering signal is known. More about the usefulness of this spectral characteristic can be found in [12].

### 3.2 Introduction of the Exponential Window

The plot of functions  $\exp(x)$  and  $I_0(x)$  (zero order Bessel function of first kind used for Kaiser window) are shown in Fig. 16. It is clear from this figure that they exhibit the same shape characteristics which is exponential in nature. For this reason, a new window which is called Exponential window is defined as:

$$w_{ex}(k) = \frac{\exp\left(\alpha_{ex}\sqrt{1 - \left(\frac{2n}{N-1}\right)^2}\right)}{\exp(\alpha_{ex})}, \quad |n| \leq \frac{N-1}{2} \quad (3-6)$$

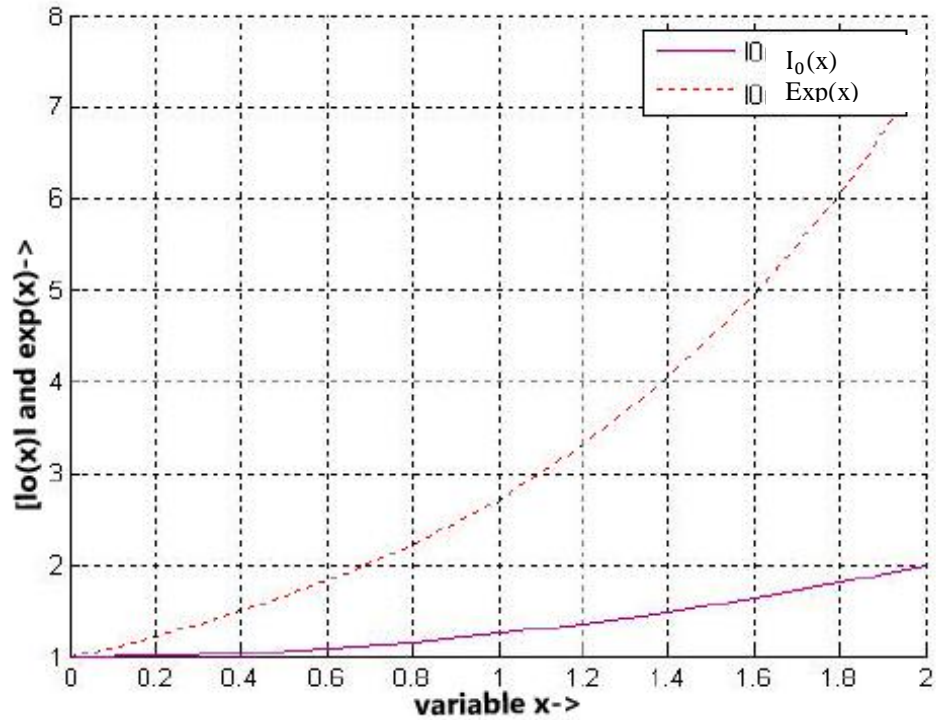


Figure 16: The Functions exp(x) and I<sub>0</sub>(x) Characteristics which have Similar Shape

The normalized spectrum of the Exponential window in dB can be written as:

$$W_N(e^{j\omega T}) = 20 \log_{10} \left( \frac{|A(\omega)|}{|A(\omega)|_{max}} \right) \quad (3-7)$$

The magnitude response of the Exponential window obtained with different values of  $\alpha_{ex}$  when the value of filter length is constant ( $N = 51$ ) is shown in Figure 17. It should be noted that  $\alpha_{ex}=0$  corresponds to the rectangular window. It is obvious from Fig. 17 that the mainlobe width increases and ripple ratio decreases if  $\alpha_{ex}$  is increased.



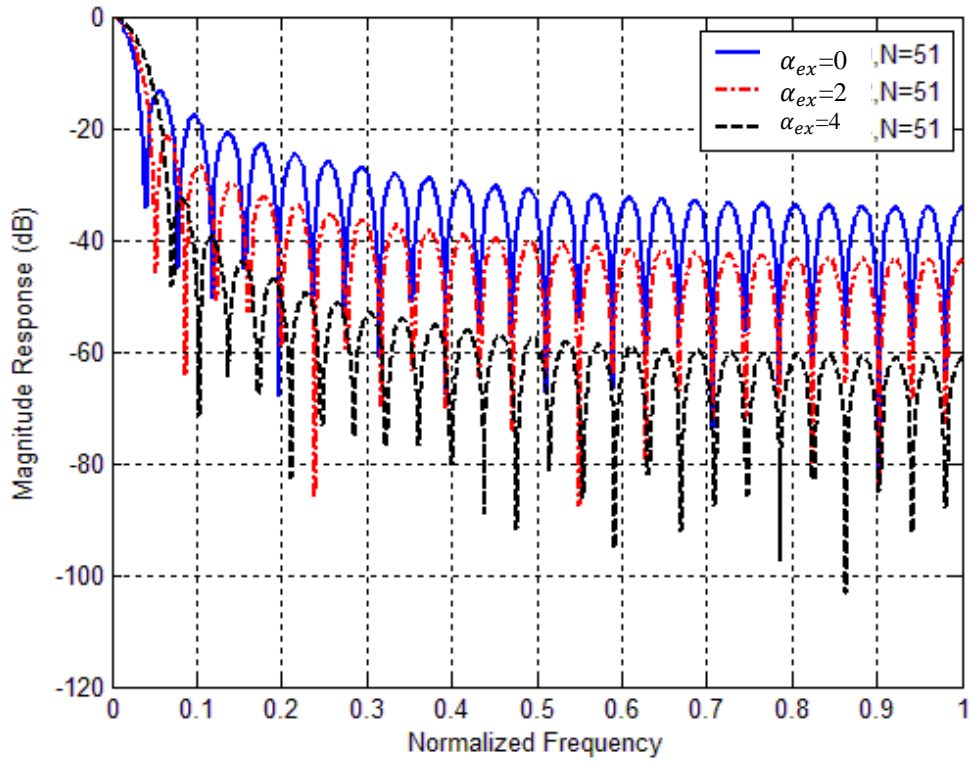


Figure 17: Proposed Window Spectrum in dB for  $\alpha_{ex}= 0, 2,$  and  $4$  and  $N=51$

### 3.3 FIR Filter Design Using Exponential Window

In designing FIR filters, the most straightforward approach is the Fourier series technique. This technique requires a very small calculation in comparison to other optimization methods. The idea of using a window in Fourier series technique is to truncate and smooth the infinite duration impulse response of the ideal prototype filter. The realizable noncausal FIR filter with a window function,  $w(nT)$ , has the following impulse response :

$$h_{nc}(nT) = w(nT)h_{id}(nT) \quad (3-8)$$

where  $h_{id}(nT)$  represents the infinite duration impulse response of the ideal filter. The infinite duration impulse response of a low pass filter (LPF) with a cut off frequency ( $\omega_c$ ) and a sampling frequency ( $\omega_s$ ) can be obtained from [1].

$$h_{id}(nT) = \left\{ \begin{array}{l} \frac{\omega_c T}{\pi} \quad ; n = 0 \\ \frac{\sin \omega_c nT}{n\pi} \quad ; \omega_c \leq |\omega| \leq \omega_s / 2 \end{array} \right\} \quad (3-9)$$

It is possible to obtain a causal filter by delaying the noncausal impulse response,  $h_{nc}(nT)$ , by period  $(N - 1)/2$ . The expression of this causal filter is given by:

$$h(nT) = h_{nc} \left[ \left( n - \frac{N - 1}{2} \right) T \right] ; 0 \leq n \leq N - 1 \quad (3-10)$$

It is well known that the filters which are designed by the window method have approximately equal ripples in the passband and stopband regions [6]. Fig. 18 shows the magnitude response of digital FIR filter designed by exponential window. The parameter ( $\alpha_{ex}$ ) effect on the filter characteristic can be clearly noticed. Also, it is clear from Fig. 18 that when  $\alpha_{ex}$  is increased, the minimum stopband attenuation ( $A_s$ ) becomes better but the transition width becomes worse.

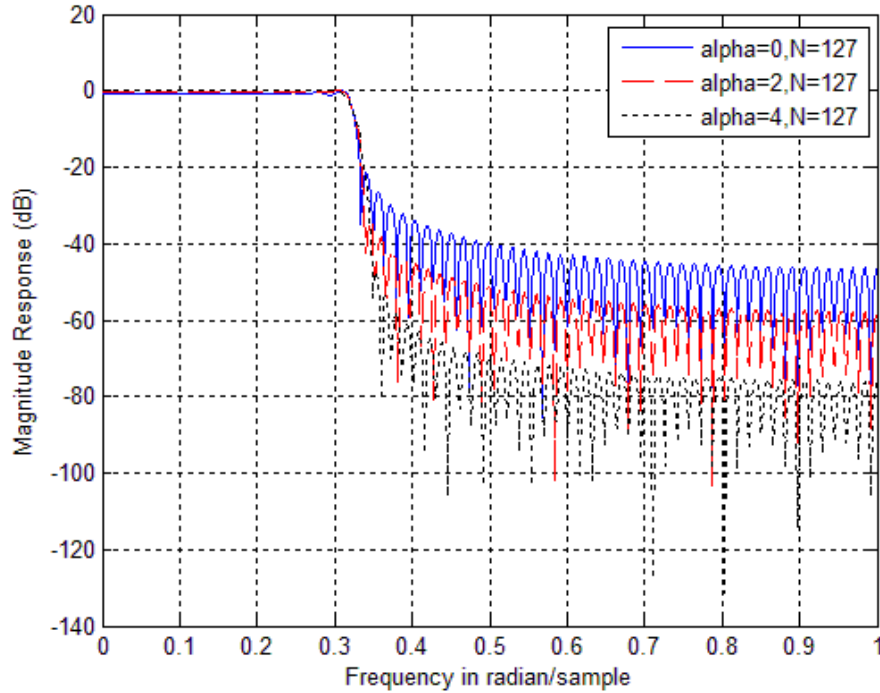


Figure 18: Amplitude Spectrums of the Filters Designed by the Exponential Window for Various Alpha with N=127

### 3.4 Filter Design Using Exponential Window Function

In order to find an appropriate window satisfying desired filter specifications, it is needed to find the relationship between the window parameters and the filter parameters. The relationship between Exponential window parameter,  $\alpha_{ex}$  and the minimum stopband attenuation ( $A_s$ ) has been shown in Fig. 19 when  $N=127$ . It is obvious from Fig. 19 that the value of minimum stopband attenuation increases when the value of the window parameter becomes larger. The first design equation which can be obtained by applying the quadratic polynomial curve fitting method can be written as:

$$\alpha_{ex} = -0.0004275 A_s^2 + 0.1808 A_s - 3.516 \quad ; A_s \leq 20.77 \quad (3-11)$$

Secondly, in filter design equation, in order to find the minimum length of the filter, the relation between the normalized width,  $D$ , and the minimum stopband attenuation ( $A_s$ ) should be obtained [7]. Also, the equation of the normalized width parameter can be written as:

$$D = \frac{\Delta\omega(N - 1)}{\omega_s} \quad (3-12)$$

where  $\Delta\omega$  denotes the transition bandwidth.

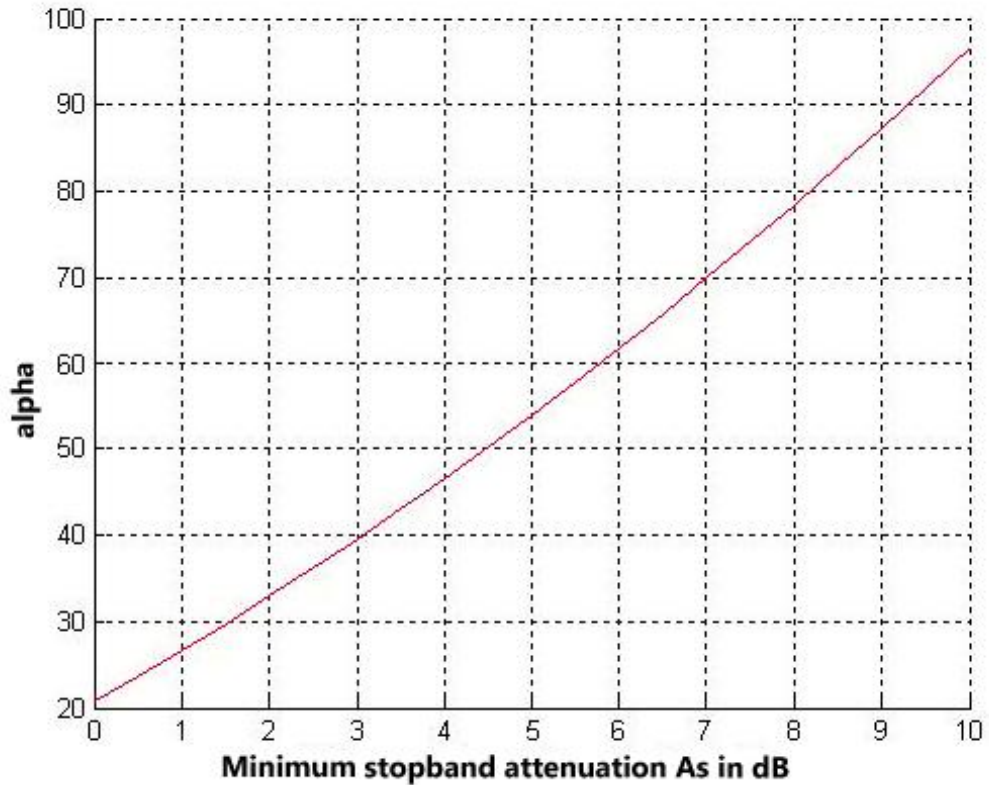


Figure 19: The Relation between Alpha and the Minimum Stopband Attenuation for Exponential Window with  $N=127$

Fig. 20 shows the relation between the stopband attenuation ( $A_s$ ) and the normalized width ( $D$ ). A comparison is also shown in Fig. 20 between the filters designed by Kaiser and Exponential windows. It can be seen from Fig. 20 that the filters designed by Kaiser window exhibit better minimum stopband attenuation characteristic than that of designed by exponential window. An approximate equation for the normalized width ( $D$ ) can be determined by using quadratic curve fitting method as follows

$$D = 5.188 \times 10^{-5} A_s^2 + 0.06617 A_s - 0.1518 \quad ; \quad A_s \leq 20.77 \quad (3-13)$$

The minimum odd integer filter length needed to satisfy  $A_s$  and  $\Delta\omega$  can be obtained, with the help of equations (3-12) and (3-13),

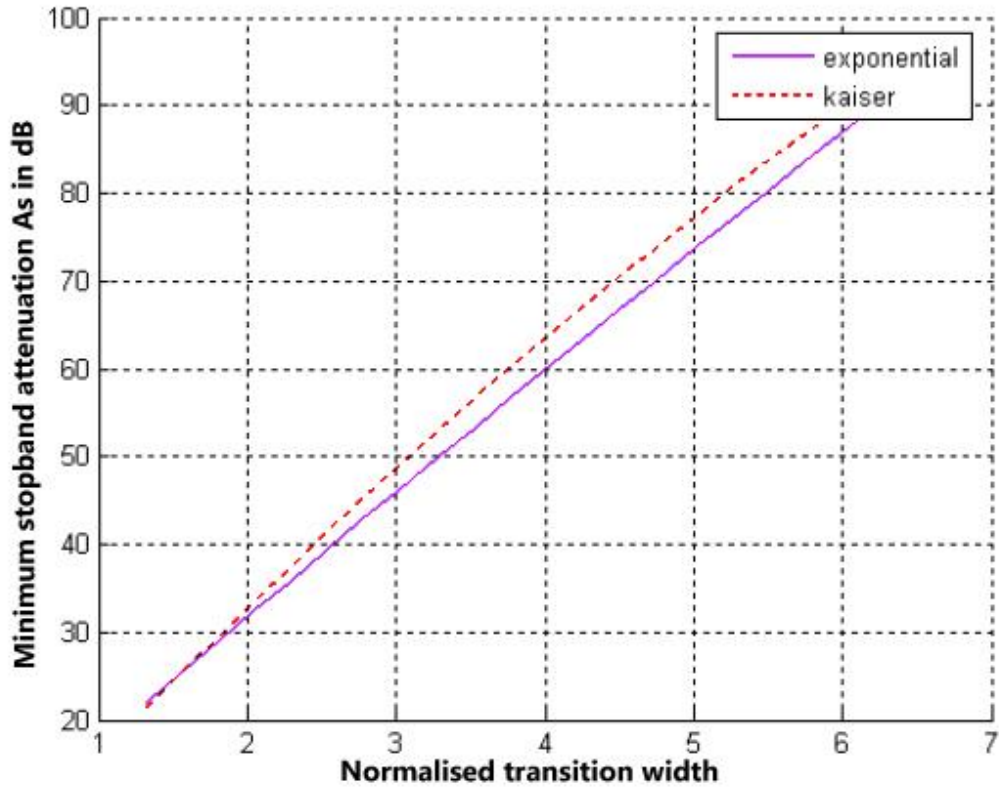


Figure 20: The Difference in the Minimum Stopband Attenuation with  $N=127$  between the Filters Designed by Exponential and Kaiser Windows

As a consequence, an exponential window can be designed by using equations (3-11), (3-12) and (3-13). It is worth to note that this exponential window is expected to satisfy the desired filter characteristic presented in terms of  $\Delta\omega$  and  $A_s$ .

In order to do another comparison with Kaiser window, the far end stopband attenuation is also considered as a figure of merit. Fig. 21 shows the comparison of far end stopband attenuation in FIR filter which is designed by exponential and Kaiser windows. It is obvious from Fig. 21 that when the transition width is increased, the filters designed by exponential window provide better far end suppression than that of designed by Kaiser window.

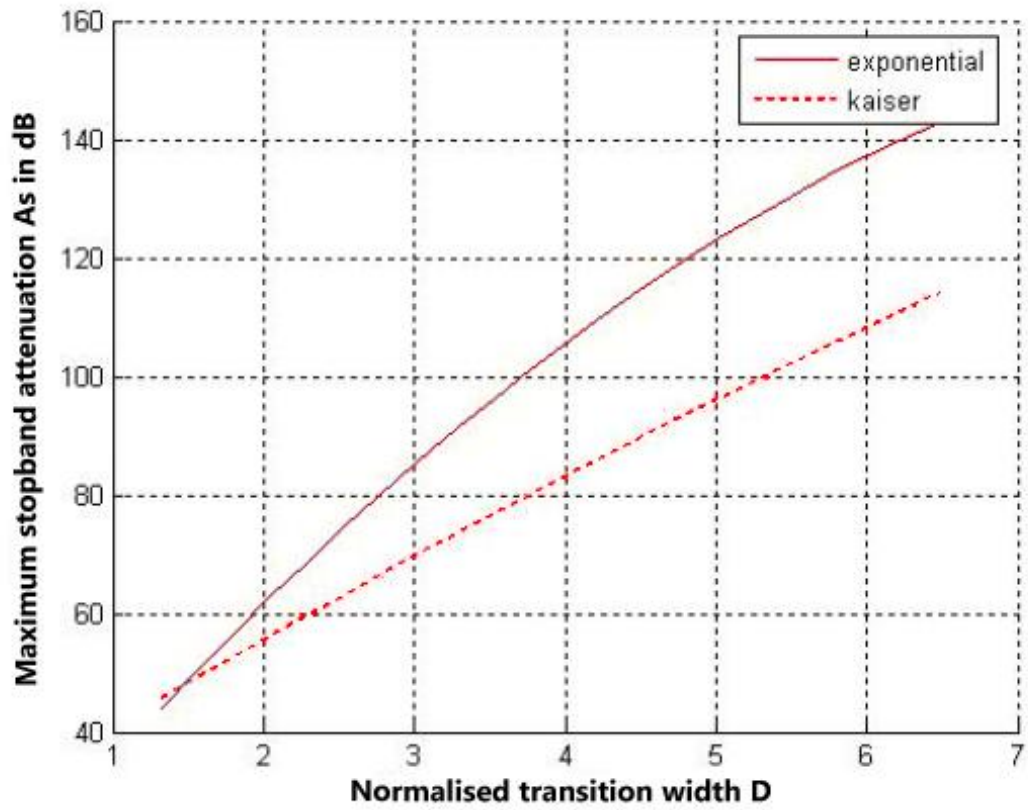


Figure 21: The Difference between the Designed Filters once when Exponential and Kaiser windows, the term of Comparison is the Maximum Stopband Attenuation with  $N=127$

## Chapter 4

### COMPUTER SIMULATIONS

In this chapter, the simulation results carried out for designing a lowpass FIR filter by using Kaiser, Cosh, and Exponential windows satisfying the following specifications are discussed:

Sampling frequency  $F_s=5$  kHz,

passband edge frequency=100 Hz,

stopband edge frequency=150 Hz,

passband attenuation=10 dB,

stopband attenuation=60 dB,

## 4.1 FIR Filter Design by Kaiser Window

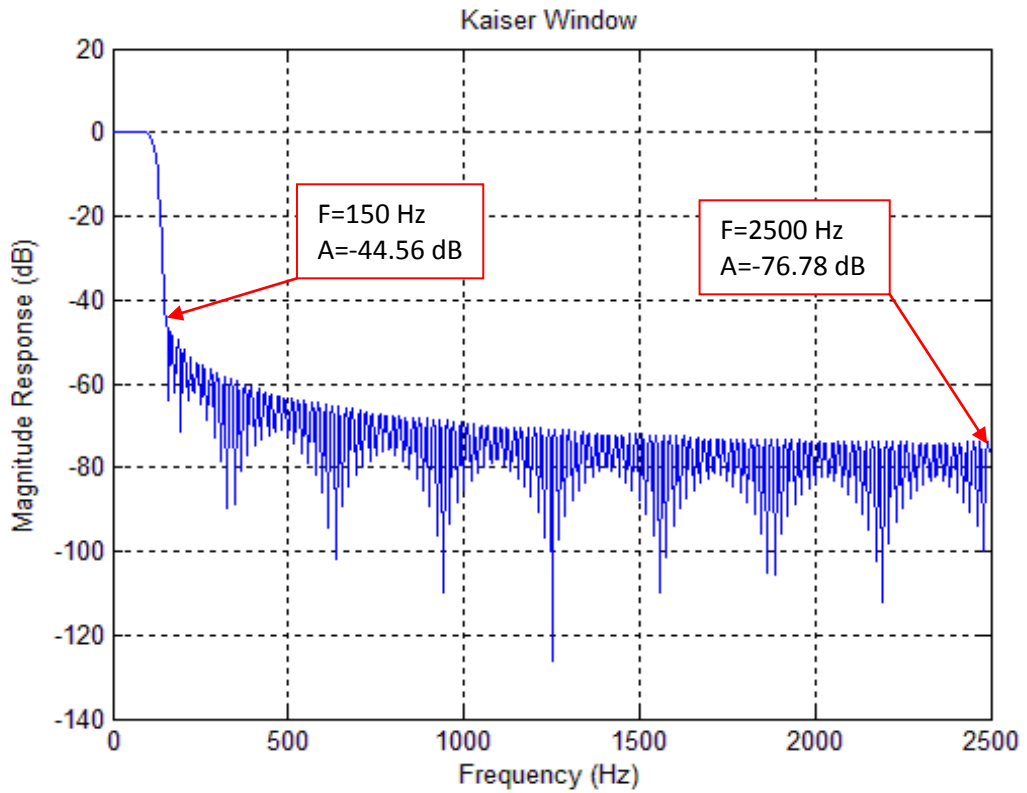


Figure 22: Frequency Response of FIR Filter Obtained by Kaiser Window, where F=frequency and A=magnitude

Fig. 22 shows the simulated frequency response of the FIR filter which is designed by the Kaiser window. To achieve a 50 Hz transition band (from 100 to 150 Hz) and at least 50 dB of attenuation (from 10 to 60 dB) in the design, the value of  $\alpha_k$  was taken as 3.9524 and the number of coefficients (filter length) was taken as  $N = 259$ . The far end stopband attenuation (FSA) is measured as  $FSA = -76.78\text{dB}$  and the minimum stopband attenuation (MSA) was measured as  $MSA = -44.56\text{dB}$ .



## 4.2 FIR Filter Design by Cosh Window

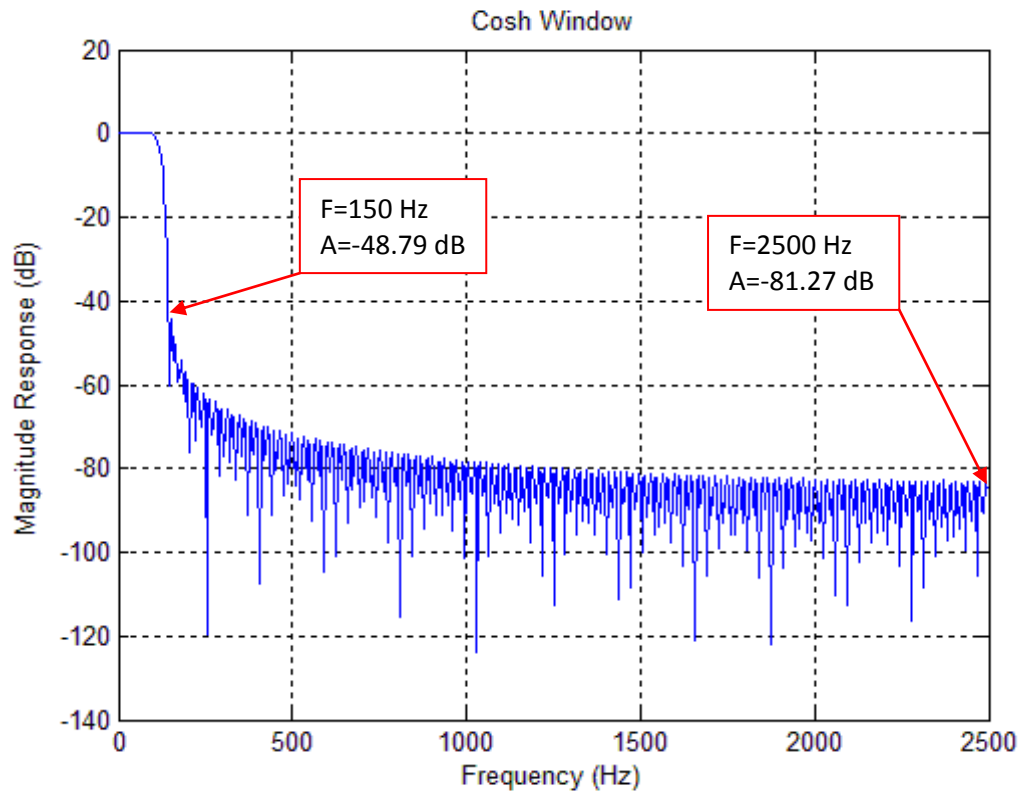


Figure 23: Frequency Response of FIR Filter Obtained by Cosh Window, where F=frequency and A=magnitude

Fig. 23 shows the frequency response of the FIR filter which is designed by the Cosh window. To achieve a 50 Hz transition band (from 100 to 150 Hz) and at least 50 dB of attenuation (from 10 to 60 dB) in the design, the value of  $\alpha_c$  was taken as 3.7111 and the number of coefficients was set to  $N = 295$ . The far end stopband attenuation is measured as  $FSA = -81.27\text{dB}$  and the minimum stopband attenuation was measured as  $MSA = -48.79\text{dB}$ .

### 4.3 FIR Filter Design by Exponential Window

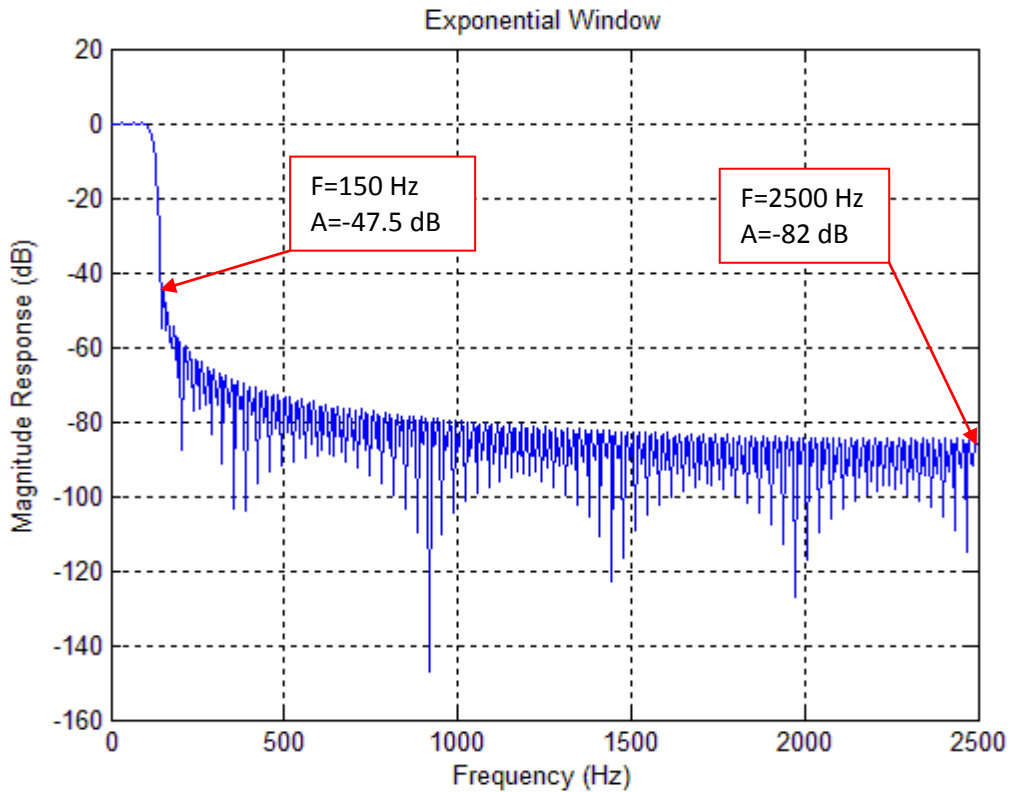


Figure 24: Frequency Response of FIR Filter Obtained by Exponential Window, where F=frequency and A=magnitude

Fig. 24 shows the frequency response of the FIR filter which is designed by the Exponential window. To achieve a 50 Hz transition band (from 100 to 150 Hz) and at least 50 dB of attenuation (from 10 to 60 dB) in the design, the value of  $\alpha_{ex}$  was taken as 3.7254 and the number of coefficients was set to  $N = 293$ . The far end stopband attenuation is measured as FSA=-82dB and the minimum stopband attenuation was measured as MSA=-47.5dB.

Table 2: Comparison of FIR Filters Designed by Kaiser, Cosh and Exponential Windows

<b>Parameters</b>	<b>Kaiser</b>	<b>Cosh</b>	<b>Exponential</b>
$\omega_c$	0.7695	0.7695	0.7695
D	2.5659	2.9329	2.9165
Alpha ( $\alpha$ )	3.9524	3.7111	3.7254
N	259	295	293
FSA (in dB)	-76.78	-81.27	-82
MSA ( in dB)	-44.56	-48.79	-47.5

The parameters of Kaiser, Exponential and Cosh windows together with the FSA and MSA values obtained from the simulation study are recorded in Table 2. The normalized cutoff frequency ( $\omega_c$ ) is computed by using the following equation

$$\omega_c = 2 \times \pi \times f_c \quad (4-1)$$

where  $f_c$  is a cutoff frequency. Normalized transition width (D) is computed by using the following equation

$$D = \frac{\Delta\omega(N - 1)}{\omega_s} \quad (4-2)$$

where  $\Delta\omega$  is a transition bandwidth, (N) is a filter length and  $\omega_s$  is sampling frequency. From table 2, it is obvious that the Exponential window provides maximum FSA than that of obtained by Kaiser and Cosh windows. However, its performance in the minimum stopband is not the best. Here, the Kaiser window provides maximum MSA than that of obtained by Exponential and Cosh windows [13].

#### 4.4 Performance Comparison of the Filters

Performances of the FIR filters designed by the Exponential, Kaiser and Cosh window functions were tested by applying a sinusoidal input,  $x(n)$ , with a frequency of 50 Hz and inspecting the output produced by the filter.

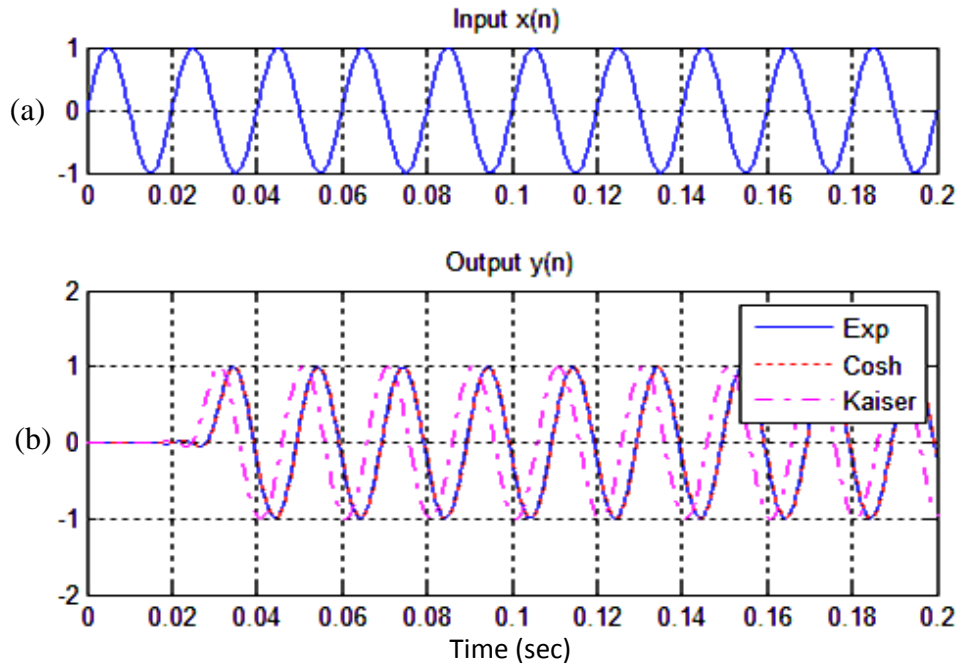


Figure 25: (a) Sinusoidal Input, (b) Outputs of the Filter Obtained by Kaiser, Cosh and Exponential windows

Fig.25 shows the input signal and the output signals obtained from the filter designed by Kaiser, Cosh and Exponential windows. Since the frequency of the input signal is 50Hz which is within the passband of the filter whose magnitude response is equal to one, the amplitude of the output signal remains unchanged for all window functions. However, there exists a phase shift between input and output due to the characteristics of the filter.

Again, performances of the same FIR filters were tested by applying a sinusoidal input,  $x(n)$ , with a frequency of 150 Hz and inspecting the output produced by each filter.

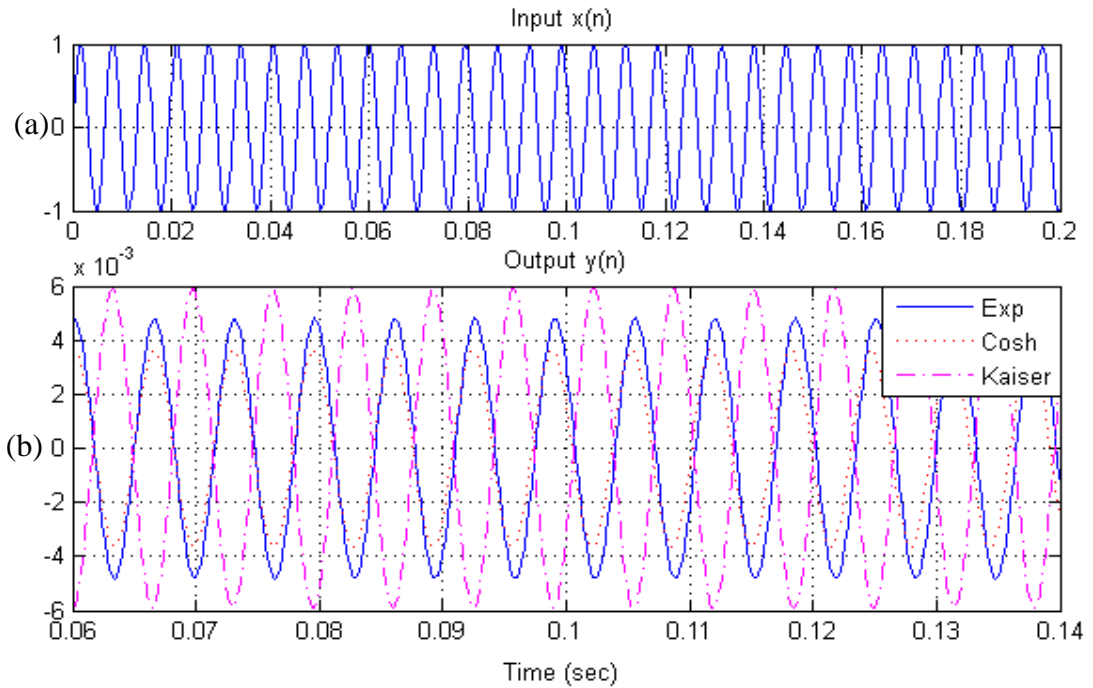


Figure 26: (a) Sinusoidal Input, (b) Outputs of the Filter Obtained by Kaiser, Cosh and Exponential windows

Fig.26 shows the input signal and the output signals obtained from each filter. The frequency of the input signal is 150Hz which is the cut-off frequency of the filter. The amplitude of the output signal obtained from the filter designed by Kaiser window is approximately  $6 \times 10^{-3}$  which agrees well with the result obtained from

$$10^{(-44.56/20)} = 5.915 \times 10^{-3} \quad (4-3)$$

where 44.56 is the MSA value in dB at 150Hz (see Fig. 22).

Similarly, the amplitude of the output signal obtained from the filter designed by Cosh window is approximately  $3.6 \times 10^{-3}$  which agrees well with the result obtained from

$$10^{(-48.79/20)} = 3.634 \times 10^{-3} \quad (4-4)$$

where 48.79 is the MSA value in dB at 150Hz (see Fig. 23).

Finally, the amplitude of the output signal obtained from the filter designed by Exponential window is approximately  $4.4 \times 10^{-3}$  which agrees well with the result obtained from

$$10^{(-47.5/20)} = 4.216 \times 10^{-3} \quad (4-5)$$

where 47.5 is the MSA value in dB at 150Hz (see Fig. 24).

The far end stopband attenuation performance of the filters can also be tested by selecting the frequency to be in the stopband (i.e. beyond the cutoff). It is clear from table2 that the amplitude of the output signal obtained from the filter designed by the Exponential window is expected to be the minimum compared with the outputs of other filters. This shows that the performance of the Exponential window is the best in the far end stopband.

## Chapter 5

### CONCLUSIONS

The application of the Exponential window in the nonrecursive digital FIR filter design has been introduced in this thesis. It has been observed that the Exponential window exhibits worse minimum stopband attenuation than that of obtained by Kaiser Window. However, it offers better far end attenuation than the filter which is designed by Kaiser and Cosh windows. Comparisons are based on the normalized transition width, filter length, design parameter, far end stopband attenuation and minimum stopband attenuation. The better far end stopband attenuation can be considered as a significant improvement which can be used in subband coding and speech applications.

The minimum and far end stopband attenuation levels regarding each filter have been verified by a simulation study. The simulation results showed a good agreement with the theoretical results.

As a continuation of this work, the following points can be taken into consideration as a future work.

- i) Trial of higher order Bessel functions which have exponential characteristics instead of the exponential window in an attempt to improve the minimum stop band attenuation while maintaining the far end stop band attenuation improvement.

- ii) Modification of Kaiser window by adding a multiplicative exponential term which will result in improvement in both the minimum stop band attenuation and far end stop band attenuation.
- iii) Relate the delay characteristics of the filter to the far-end stop band attenuation and advise an empirical formula that can be used to automate the design procedure.



## REFERENCES

- [1] A. Antoniou, "Digital signal processing: Signal, systems, and filters", McGraw-Hill, 2005.
- [2] J. F. Kaiser and R. W. Schafer, "On the use of the Io-sinh window for spectrum analysis," IEEE Trans. Acoustics, Speech, and Signal Processing, vol. 28, no. 1, pp. 105-107, 1980.
- [3] C. L. Dolph, "A Current Distribution for Broadside Arrays Which Optimizes the Relationship Between Beamwidth and Side-lobe Level," Proc. IRE, vol. 34, pp. 335-348, 1946.
- [4] A. Jain, R. Saxena and S. C. Saxena, "A simple alias-free QMF system with near-perfect reconstruction," J. Indian Ins. Sci., no. 12, pp. 1-10, 2005.
- [5] T. Saramaki, "A class of window functions with nearly minimum sidelobe energy for designing FIR filters," in Proc. IEEE Int. Symp. Circuit and Systems (ISCAS), vol. 1, pp. 359-362, 1989.
- [6] J. F. Kaiser, "Nonrecursive digital filter design using I0-sinh window function," in Proc. IEEE Int. Symp. Circuits and Systems (ISCAS'74), pp. 20-23, 1974.
- [7] S. W. Bergen and A. Antoniou, "Design of ultraspherical window functions with prescribed spectral characteristics," EURASIP Journal on Applied Signal

Processing, no. 13, pp. 2053-2065, 2004.

- [8] K. Avci and A. Nacaroglu, "A New Window Based on Exponential Function," in Proc. of 3rd International Conference on Information & Communication Technologies: From Theory to Applications (ICTTA'08), Damascus, Syria, 2008.
- [9] B. A. Shenoi, "Introduction to digital signal processing and filter design," 2006, pp. 251-258.
- [10] E. C. Ifeachor and B. W. Jervis , "Digital signal processing: a practical approach", Prentice Hall, Second ed., 2002.
- [11] H. H. Monson , "Schaum's Outline of Theory and Problems of Digital Signal Processing", 1999.
- [12] F. J. Harris, "On the use of windows for harmonic analysis with the discrete Fourier transform," Proc. of the IEEE, pp. 51-83, 1978.
- [13] V. Soni, P. Shukla and M. Kumar, "Application of Exponential window to design a digital nonrecursive FIR filter," in proc. 13<sup>th</sup> International Conference on Advanced Communication technology (ICACT), , pp. 1015-1019. IEEE, 2011.

## **APPENDICES**

## Appendix A1: Simulations of FIR Filter Design by Exponential, Kaiser and Cosh Window

```
clc;
clear
disp('for Exponential Window choose      1');
disp('for Kaiser Window choose          2');
disp('for Cos hyperbolic Window choose   3');
windowtype=input('window type=');
fs=5000;
if windowtype==1
    alpha=3.7254;
    N=293;
    w=expwin(N+1,alpha);
    h=fir1(N,0.05,w);
    [H,f] = freqz(h,1,512,fs);
    mag = 20*log10(abs(H));
    plot(f,mag), grid on;
    title('Exponential Window');
    xlabel ('Frequency in Hertz')
    ylabel ('MagnitudeResponse(dB)')
elseif windowtype==2
    alpha=3.9524;
    N=259;
    w=kaiser(N+1,alpha);
    h=fir1(N,0.05,w);

    [H,f] = freqz(h,1,512,fs);
    mag = 20*log10(abs(H));
    plot(f,mag), grid on
    title('Kaiser Window');
    xlabel ('Frequency in Hertz')
    ylabel ('MagnitudeResponse(dB)')
else
    alpha=3.7111;
    N=295;
    w=coshwin(N+1,alpha);
    h=fir1(N,0.05,w);

    [H,f] = freqz(h,1,512,fs);
    mag = 20*log10(abs(H));
    plot(f,mag), grid on
    title('Cosh Window');
    xlabel ('Frequency in Hertz')
    ylabel ('MagnitudeResponse(dB)')

end

% % %=====End=====% % %
```

## Function for Exponential and Cosh Window

```
function w = expwin(n_est,bta)
error(nargchk(1,2,nargin,'struct'));
if nargin < 2 || isempty(bta),
    bta = 0.000;
end
[nn,w,trivialwin] = check_order(n_est);
if trivialwin, return, end;
nw = round(nn);
bes = abs(cosh(bta));
odd = rem(nw,2);
xind = (nw-1)^2;
n = fix((nw+1)/2);
xi = (0:n-1) + .5*(1-odd);
xi = 4*xi.^2;
w = cosh(bta*sqrt(1-xi/xind))/bes;
w = abs([w(n:-1:odd+1) w])';

function [n_out, w, trivalwin] = check_order(n_in)
w = [];
trivalwin = 0;

if ~(isnumeric(n_in) & isfinite(n_in)),
    error(message('signal:check_order:InvalidOrderFinite', 'N'));
end
if n_in < 0,
    error(message('signal:check_order:InvalidOrderNegative'));
end
if isempty(n_in) | n_in == floor(n_in),
    n_out = n_in;
else
    n_out = round(n_in);
    warning(message('signal:check_order:InvalidOrderRounding'));
end
if isempty(n_out) | n_out == 0,
    w = zeros(0,1);
    trivalwin = 1;
elseif n_out == 1,
    w = 1;
    trivalwin = 1;
end
end
```

## Appendix A2: Performance Comparison of the Filters

```
%% Exponential Window%%
clc;
clear
M=58;
A=1;
fc=122.47;
f=input('Enter the Frequency = ');
w=2*pi*f;
theta=0;
fs=5000;
n=0:1/fs:0.2;
x=A*sin((w*n)+theta);
subplot(3,1,1);
plot(n,x);
title('Input x(n) ');
grid

alpha=3.7254;
N=293;
w=expwin(N+1,alpha);
h=fir1(N,fc/fs*2,w);
[H,f] = freqz(h,1,512,fs);
mag = 20*log10(abs(H));
y=filter(h,1,x);
subplot(3,1,2);
plot(n,y);
title('Output y(n)');
grid

[H,f]=freqz(h,1,512,fs);
mag=20*log10(abs(H));
subplot(3,1,3);
plot(f,mag);
title(' Output filter ');grid
xlabel ('Frequency (Hz)')

% % %=====End===== % % %

%%Cosh Window%%
clc;
clear
M=58;
A=1;
fc=122.47;
f=input('Enter the Frequency = ');
w=2*pi*f;
theta=0;
fs=5000;
n=0:1/fs:0.2;
x=A*sin((w*n)+theta);
subplot(3,1,1);
plot(n,x);
title('Input x(n) ');
grid

alpha=3.7111;
N=295;
```

```

w=coshwin(N+1,alpha);
h=fir1(N,fc/fs*2,w);
[H,f] = freqz(h,1,512,fs);
mag = 20*log10(abs(H));
y=filter(h,1,x);
subplot(3,1,2);
plot(n,y);
title('Output y(n)');
grid

[H,f]=freqz(h,1,512,fs);
mag=20*log10(abs(H));
subplot(3,1,3);
plot(f,mag);
title(' Output filter ');grid
xlabel ('Frequency (Hz)')

% % %=====End===== % % %

%%Kaiser Window%%
clc;
clear
M=58;
A=1;
fc=122.47;
f=input('Enter the Frequency = ');
w=2*pi*f;
theta=0;
fs=5000;
n=0:1/fs:0.2;
x=A*sin((w*n)+theta);
subplot(3,1,1);
plot(n,x);
title('Input x(n) ');
grid

alpha=3.9524;
N=259;
w=kaiser(N+1,alpha);
h=fir1(N,fc/fs*2,w);
[H,f] = freqz(h,1,512,fs);
mag = 20*log10(abs(H));
y=filter(h,1,x);
subplot(3,1,2);
plot(n,y);
title('Output y(n)');
grid

[H,f]=freqz(h,1,512,fs);
mag=20*log10(abs(H));
subplot(3,1,3);
plot(f,mag);
title(' Output filter ');grid
xlabel ('Frequency (Hz)')
% % %=====End===== % % %

```